Analysis for BrO in zenith-sky spectra: An intercomparison exercise for analysis improvement

S. R. Aliwell,[1] M. Van Roozendael,[2] P. V. Johnston,[3] A. Richter,[4] T. Wagner,[5] D. W. Arlander,[6] J. P. Burrows,[4] D. J. Fish,[7] R. L. Jones,[1] K. K. Tørnkvist,[6] J.-C. Lambert,[2] K. Pfeilsticker,[5] and I. Pundt [5,8]

Received 4 January 2001; revised 26 June 2001; accepted 27 June 2001; published 20 July 2002.

[1] The analysis for BrO using the technique of differential optical absorption spectroscopy as applied to spectra of light scattered from the zenith sky has historically presented something of a challenge, leading to uncertainty about the accuracy of measurements. This has largely been due to the large sensitivity of the measurement to many analysis parameters and due to the small size of the absorption features being measured. BrO differential slant columns have been measured by six different groups taking part in an intercomparison exercise at Observatoire de Haute-Provence in France from 23 to 27 June 1996. The data are analyzed in a collaborative attempt to improve the overall analysis for BrO through investigation of a series of sources of errors in the instrumentation, calibration, input to the analysis, and the spectral analysis itself. The study included comprehensive sensitivity tests performed using both actual measurements and synthetic data. The latter proved invaluable for assessing several aspects of the spectral analysis without the limitations of spectral quality and instrument variability. The most significant sources of error are identified as the wavelength calibration of several of the absorption cross sections fitted and of the measured spectra themselves, the wavelength region of the fitting, the temperature dependence of the O_3 absorption cross sections, failure to adequately account for the so-called I_0 effect, inadequate offset correction, and inadequate measurement of the individual instrument slit functions. Recommendations for optimal analysis settings are presented, and comparing the results from the analysis of the campaign data shows BrO differential slant column observations from the various groups to be in agreement to within 4% on average between 87° and 90° solar zenith angle, with a scatter of 16%. *INDEX TERMS:* 0340 Atmospheric Composition and Structure: Middle atmosphere—composition and chemistry; 0365 Atmospheric Composition and Structure: Troposphere—composition and chemistry; 0394 Atmospheric Composition and Structure: Instruments and techniques; 1610 Global Change: Atmosphere (0315, 0325); *KEYWORDS:* bromine, monoxide, optical, absorption, spectroscopy

1. Introduction

[2] A number of studies of BrO measured by ground-based zenith-sky spectroscopy at middle and high latitudes have been reported [e.g., *Carroll et al.*, 1989; *Arpag et al.*, 1994; *Fish et al.*, 1995; *Eisinger et al.*, 1997; *Aliwell et al.*, 1997; *Kreher et al.*, 1997; *Otten et al.*, 1998]. The analysis for BrO by the technique of differential optical absorption spectroscopy (DOAS) as applied to spectra of light scattered from the zenith sky is a difficult measurement owing to the small absorption of BrO relative to the other absorbers in the same wavelength region (especially O_3) and thus requires considerable attention to the detail of the analysis. The measurement is somewhat easier in polar regions during winter when NO_2 and O_3 are at significantly lower concentrations than at midlatitudes and the interference in the analysis is thus reduced [e.g., *Kreher et al.*, 1997]. Additionally, the temperature dependence of the O_3 cross section is less marked at the lower temperatures. Small discrepancies between values for BrO measured in situ on board airplanes or balloons [e.g., *Brune and Anderson*, 1986; *Avallone et al.*, 1995; *McKinney et al.*, 1997] and ground-based [e.g., *Arpag et al.*, 1994; *Fish et al.*, 1995, 1997; *Eisinger et al.*, 1997] or balloon-borne UV-visible measurements [*Harder et al.*, 1998; *Pundt et al.*, 2000] point to the need for an examination of the accuracies of the

[1]Centre for Atmospheric Science, University of Cambridge, Cambridge, UK.
[2]Institut d'Aéronomie Spatiale de Belgique, Brussels, Belgium.
[3]National Institute of Water and Atmospheric Research, Omakau, Central Otago, New Zealand.
[4]Institute of Environmental Physics, University of Bremen, Bremen, Germany.
[5]Institute of Environmental Physics, University of Heidelberg, Heidelberg, Germany.
[6]Norwegian Institute for Air Research, Kjeller, Norway.
[7]Department of Meteorology, University of Reading, Reading, UK.
[8]Service d'Aéronomie du CNRS, Verrières-le-Buisson, France.

0148-0227/02/2001JD000329$09.00

Table 1. Summary of Participating Instrument Characteristics as Set Up for Measuring BrO at Observation de Haute Provence During June 1996

Group	UCam	Bremen	Heidelberg	NIWA	NILU	IASB
Spectral range, nm	320–385	325–405	308–403	336–390	332–482	339–406
Resolution, nm/FWHM	0.7	0.8	0.6	0.7	0.9	0.6
Sampling ratio, pix/FWHM	12	10	6	11.5	6	9
Detector type	Charge-coupled device	Reticon diode array	Reticon diode array	photomultiplier tube	NMOS diode array	Reticon diode array
Detector temperature, °C	−55	−40	−32	32	−30	−38
Temperature stabilized	yes	yes	yes	yes	no	yes
Field of view, deg full angle	<1	<1	0.2	12	16	2
Filter	yes	yes	yes	no	no	no
Light delivery	mirrors, f/4 lens	fiber bundle	fiber bundle	mirrors	fiber bundle	fiber bundle
Polarization response accounted for	no	fiber depolarizes	fiber depolarizes	polarization tracked, polarizer filter	fiber depolarizes	fiber depolarizes
References	*Aliwell et al.* [1997]	*Richter* [1997]	*Otten et al.* [1998]		*Tørnkvist et al.* [2002]	*Van Roozendael et al.* [1998]

analysis techniques. In addition, any coordinated measurement campaign requires that the instruments be shown to retrieve similar values under similar conditions.

[3] An intercomparison exercise was held at Observatoire de Haute-Provence (OHP) (43.9°N, 5.7°E) in France from 23 to 27 June 1996 in order to gather measurements for an analysis workshop to be held later. The conditions were not ideal for a BrO intercomparison, resulting in relatively low differential slant columns of BrO when compared to most middle and high latitude studies due to lower latitude and midsummer conditions. However, this time and place were chosen in order to take advantage of the presence of a number of instruments taking part in a Network for Detection of Stratospheric Change (NDSC) NO_2 and O_3 measurement intercomparison [*Roscoe et al.*, 1999]. In contrast to the NDSC intercomparison, the BrO exercise had no level of blind intercomparison but was rather an opportunity to improve the analysis for each group by consensus and to highlight the sources of errors in the instrumentation, calibration, input to the analysis, and the spectral analysis itself. The groups contributing measurements were University of Cambridge (UCam), University of Bremen (Bremen), University of Heidelberg (Heidelberg), National Institute of Water and Atmospheric Research (NIWA), Norwegian Institute for Air Research (NILU), and Institut d'Aéronomie Spatiale de Belgique (IASB). Service d'Aeronomie du CNRS (CNRS) and Heidelberg make balloon-borne measurements of BrO using UV-visible type spectrometers that employ a DOAS technique similar to the ground-based measurements groups [*Pundt*, 1997; *Pundt et al.*, 2000; *Harder et al.*, 1998]. Such measurements were not part of the measurement intercomparison; however, CNRS did contribute analysis of synthetic spectra.

[4] What follows is a detailed analysis of several factors aimed at improving the analysis for BrO in zenith-sky spectra. A brief discussion of the actual measurements made is presented along with a preliminary analysis that highlights the scope of the problem. This is followed by the analysis of a set of synthetic spectra that allows the testing of a variety of effects without the constraints of spectral quality and differences in ability to accurately wavelength calibrate the measured spectra. These tests isolate the analysis parameter effects from the individual instrument effects. A comprehensive set of sensitivity studies were then carried out on actual measured spectra, thus allowing an optimization of the agreed analysis parameters and a measurement of each instrument's sensitivity to particular parameters. The agreed analysis parameters (summarized as recommendations for quick reference) were then used as the basis for comparing all spectral measurements over the intercomparison period.

2. Instrumentation

[5] All participating instruments are of the UV-visible zenith-sky viewing type used in the DOAS technique. A summary of each instrument's characteristics is given in Table 1. The instruments, as set up to measure BrO, are oversampled with resolutions ranging from 0.6 to 0.9 nm. This compromise between resolution and sampling in each case gives a reasonable sensitivity to the vibrational absorption structures of BrO as well as minimizing interpolation errors and allowing a reasonable wavelength range to be measured. Temperature stabilization of instruments also helps to minimize drifts in wavelength calibration and changes in instrumental line shape. Further details of the individual instruments can be found in the relevant references given in Table 1.

3. Measurements at OHP

[6] Spectra were recorded by each group in the UV for the twilight periods of 23–27 June 1996 and were analyzed for BrO in terms of slant column differences between a particular solar zenith angle (SZA) and the reference spectrum. Differential slant columns are the natural product of the zenith-sky DOAS technique and have generally been reported as such in previous studies on BrO because of the significant uncertainties in the vertical profile of BrO that would affect the conversion to vertical column amounts [*Fish et al.*, 1995]. A reference spectrum measured by each instrument for each twilight period at a solar zenith angle of 70° was agreed upon. This is lower than the 80° reference that has generally been used for midlatitude measurements

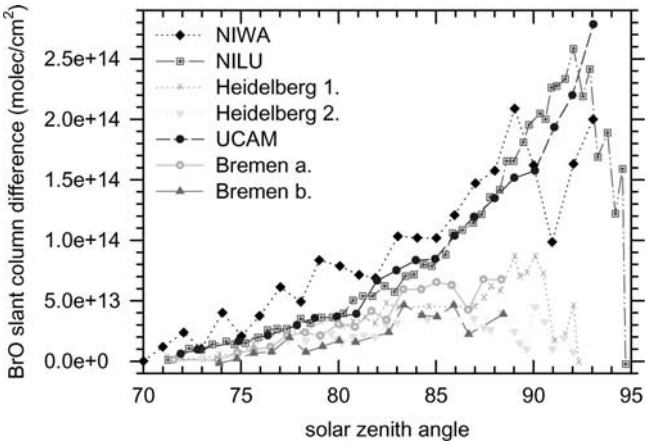

Figure 1. Comparison of the initial analyzed BrO slant column differences for the evening twilight of 26 June 1996 at Observatoire de Haute-Provence (OHP). Analysis used groups' preferred parameters. Some groups gave two different analyses. (Read 2.5e + 14 as 2.5×10^{14}, etc.)

[e.g., *Arpag et al.*, 1994; *Fish et al.*, 1995; *Eisinger et al.*, 1997; *Richter et al.*, 1999] and was chosen to maximize the differential BrO absorption since it is expected that at this lower latitude and in summer, there will be significantly less BrO than measured in previous midlatitude winter studies. This choice of reference spectrum, more separated in time from the spectra to be analyzed, may have some disadvantages. The greater time difference gives more opportunity for spectral drift in wavelength so that larger shift and stretch parameters may need to be applied with the attendant increase in noise from interpolation. In addition, the hot weather generally experienced at OHP during the time when the reference spectrum was measured will contribute to greater instability in the wavelength registration and also possibly to increased dark current where detector cooling systems struggle to maintain temperature.

4. Preliminary Analysis

[7] As a starting point, all participants were asked to analyze their data using the 70° reference spectrum and their preferred analysis specifications (e.g., cross sections or wavelength regions) and to submit results for an initial comparison. First analyses showed a considerable scatter between the various groups (for an example, see Figure 1). Analysis is very sensitive to the quality of the spectra, so the analyses presented here are not necessarily representative of measurements presented previously by the various groups involved. Most previous measurements have been made at higher latitude and in winter when the spectra were of better quality and more BrO was present, making the analysis a somewhat easier task. Figure 1 is included to show the differences possible when not performing an optimum analysis using the same conditions as others.

[8] There are a number of areas where there is potential for discrepancies in the results from the various groups. These include differences in the analysis parameters where there is considerable sensitivity to such parameters and differences in the measurements themselves. Sections 5–7 are aimed at assessing the extent to which these factors may influence the differences in retrieved BrO and, therefore, are also aimed at improving the analysis and our understanding of it.

5. Synthetic Spectra

[9] In addition to the analysis of atmospheric spectra, a set of synthetic spectra with known amounts of various absorbers was analyzed by each group. These spectra were produced using a forward model where the Beer-Lambert law is applied to a high-resolution solar atlas [*Kurucz et al.*, 1984] using a standard set of cross sections, and the resulting transmitted intensity is smoothed to the typical instrumental resolution of 0.65 nm full width at half maximum (FWHM) (P. V. Johnston, personal communication, 1996). No noise was added to the synthetic spectra. Such analyses were found to be invaluable for assessing the effects of calibration without the limitations of spectral quality. In addition, they provided a check that each group was carrying out the analysis in the same manner, thus eliminating a further variable from the eventual intercomparison of actual measured data.

[10] The synthetic atmospheric spectra and the cross sections were provided with wavelength calibration, so this study should omit the differences between the various groups' selections of cross sections and instrument functions and therefore should concentrate on the effects of the different analysis packages. These tests may also indicate any limitations in the analysis. Analyses were carried out in the wavelength region 346–359 nm using the cross sections and wavelength calibration provided and, where applicable, using a second-order polynomial. Polynomial terms are usually applied in the DOAS technique to account for the smooth, unstructured part of the atmospheric attenuation. The choice of a relatively short wavelength interval has been commonly adopted so as to minimize the interference from adjacent O_3 bands at short wavelength and to minimize the impact of the O_4 absorption to the longer-wavelength side. The region is wide enough to incorporate two BrO bands, sufficient for the fitting process. As will be explained later in this section, the calibration was allowed to vary in some tests. Two O_3 cross sections measured at different temperatures (221 and 241 K) were fitted in order to account for the temperature dependence of the O_3 cross section over the range of temperatures covered by the altitudes at which O_3 absorbs most strongly.

[11] Both I_0-corrected cross sections and uncorrected cross sections were provided, enabling an assessment of the effects of their use. Basically, the I_0 effect arises because zenith-sky spectra and laboratory absorption cross sections are usually measured at different spectral resolutions and using different light sources. To match the resolution of zenith-sky instruments, high-resolution laboratory data are traditionally filtered using the known instrumental slit function, whereby an error is introduced because in actual measurements the spectra (and not their logarithm) have been filtered by the slit function. A detailed description of this effect and the method used in the present study to account for it in the process of convolving absorption cross sections are given in Appendix A.

[12] Table 2 shows the retrieved slant columns of the various absorbers for each group when non-I_0-corrected

Table 2. Retrieved Slant Column Difference Amounts From Analysis of Synthetic Spectra Using Non-J_0-Corrected Cross Sections and Actual Amounts Used in Constructing Synthetic Spectra[a]

	0_3 ($\times 10^{19}$) 221 K	0_3 ($\times 10^{19}$) 241 K	NO_2 ($\times 10^{16}$) 227 K	BrO ($\times 10^{14}$) 223 K
Actual	8.00	2.00	5.00	1.50
UCam	6.47	3.52	4.91	2.02
NIWA	6.51	3.48	4.93	2.00
Bremen	6.50	3.49	4.93	2.00
Heidelberg	6.35	3.68	4.93	2.02
NILU	6.50	3.49	4.93	2.00
CNRS	6.11	3.99	4.97	2.00
IASB	6.50	3.49	4.93	2.00

[a]Amounts are given in molecules per square centimeter. The fitting window was 346–359 nm. The analyzed spectrum was allowed to shift and stretch with respect to the reference spectrum to achieve the lowest residual of the fit.

cross sections were used and the wavelength calibrations of the cross sections and reference spectrum were accepted as given. The analyzed spectrum was allowed to shift and stretch with respect to the reference spectrum to minimize the residual. This provides some test of the relative convergence techniques of the groups. Also included in Table 2 are the slant column amounts used in constructing the synthetic spectra. When using uncorrected cross sections, the relative concentrations fitted by the two different ozone cross sections are incorrect, while the sum of the fitted ozone does approximately equal the sum of the two used in generating the synthetic spectrum. It appears that this effect causes an erroneously high column amount of the retrieved BrO in the non-I_0-corrected case. This is probably chiefly due to misalignment of the O_3 absorption features as a result of not including a correction for the solar I_0 effect. The fit tries to compensate for the less than optimum alignment by fitting more 241-K O_3 and less 221-K O_3. There will inevitably still be unfitted absorption features due to the inadequacies of this compensation, and should these correlate with BrO absorptions, they will be fitted as such, resulting in higher BrO. This strongly supports the arguments that inadequacies in the O_3 fit are the major source of errors in the BrO retrieval. The majority of groups are able to retrieve approximately the same values of each absorber, indicating that the analysis packages perform similarly with the given restrictions. The notable exceptions are Heidelberg and the CNRS. A different approach to the analysis by each of these groups is believed to be the cause of the differences. Heidelberg includes the fitting of a "Fraunhofer coefficient," which is a scaling factor for the log of the Fraunhofer spectrum in the log ratio forming the differential spectrum [*Wagner et al.*, 1996]. The CNRS analysis does not use polynomials for the generation of differential spectra and cross sections but instead uses Fourier transform high-pass filters (a 15-nm filter in this instance). These filters are applied over a region somewhat wider than the fitting region, and though this seems to work reasonably well for a wide fitting region, it is apparently not suitable for a narrow region as used here. CNRS is currently considering changing to the use of polynomials for the BrO analysis. Nevertheless, the BrO retrieved by both Heidelberg and CNRS is very close to that of the other groups.

[13] Table 3 summarizes the results of a number of sensitivity tests carried out by IASB on the synthetic spectra. These results are representative of those achieved by the other groups. Table 3 gives the analysis type, and reference to this is made in the discussion below. These tests essentially address the issue of the combined impact of spectral shift and solar I_0 effects on the accuracy of the BrO retrieval. Table 3 is subdivided into three classes of test cases: A-type, B-type, and C-type cases. A-type tests are for calculations using standard (non-I_0-corrected) cross sections. Analysis A2 is given in Table 2, while A1 has all

Table 3. Summary of Results of Various Analysis Tests Carried Out on Synthetic Spectra[a]

Analysis Type	Description	0_3 221 K ($\times 10^{19}$)	0_3 241 K ($\times 10^{19}$)	NO_2 227 K ($\times 10^{16}$)	BrO 223 K ($\times 10^{14}$)	Shift,[b] nm/stretch of spectrum	Shift nm/stretch of cross sections
Actual		8.00	2.00	5.00	1.50	–	–
A1	Non-I_0-corrected cross sections (CS), no shift	7.12	2.85	5.00	1.89	–	–
A2	Non-I_0-corrected CS, spectrum shifted	6.50	3.49	4.93	2.00	$4.9 \times 10^{-4}/-7 \times 10^{-5}$	–
A3	Non-I_0-corrected CS, all (linked) CS shifted	7.20	2.59	5.04	1.52	$5.0 \times 10^{-4}/-1 \times 10^{-5}$	$1.8 \times 10^{-2}/3.1 \times 10^{-3}$
B1	I_0-corrected CS, no shift	8.03	1.97	5.00	1.50	–	–
B2	I_0-corrected CS, spectrum shifted	8.04	1.96	5.00	1.50	$-4.0 \times 10^{-6}/1 \times 10^{-6}$	–
B3	I_0-corrected CS using exact scaling, no shift	8.00	2.00	5.00	1.51	–	–
C1	Same as A2, but in interval 345.9–358.9 nm	6.74	3.22	4.94	1.95	$4.6 \times 10^{-4}/-6 \times 10^{-5}$	–
C2	Same as B2, but in interval 345.9–358.9 nm	8.03	1.97	5.00	1.50	$3.0 \times 10^{-6}/1 \times 10^{-6}$	

[a]Retrieved slant column amounts are given in molecules per square centimeter. These results are based on analysis carried out by IASB.
[b]Shift and stretch values given throughout this paper are calculated according to the following formula: $\Delta\lambda$ = shift + stretch($\lambda - \lambda_0$), where $\Delta\lambda$ is the wavelength displacement applied at wavelength λ and λ_0 is the central wavelength of the fitting interval.

parameters the same as A2 but has an analysis spectrum that is not allowed to shift and stretch onto the fixed reference spectrum. Since both spectra were constructed using the same solar spectrum, it might be expected that this shift and stretch would be unnecessary. However, results show that the calibration of the spectrum applied a shift of 4.9×10^{-4} nm and a stretch of -7×10^{-5} when allowed this freedom. The reasons for this are unclear; however, it is obvious that this has a significant effect on the balance of the two O_3 cross sections fitted and on the retrieved amounts of NO_2 and BrO as well. This less restrictive analysis case is in fact a step closer to the analysis that must be performed on the measured spectra. Analysis A3 further shows that it is possible to get significantly closer to the correct BrO column amount if the non-I_0-corrected cross sections are allowed some freedom to move. In this case the cross sections are allowed to shift and stretch by the same amount to find the minimum residual of the fit. Evidently, the shift and stretch process compensates to some extent for the lack of I_0 correction. However, this compensation is not total, as the incorrect O_3 and NO_2 column amounts show. In effect, it turns out that the I_0 correction shifts the peaks of the O_3 maximum absorption so that a better match is reached. B-type analyses, which are similar to A-types but use I_0-corrected cross sections rather than uncorrected ones, evidently lead to much improved results. Still, small discrepancies between the actual and retrieved O_3 columns are observed with the B1 and B2 analyses. Further tests showed that this was largely due to the fixed scaling factor used in the I_0 correction of the cross sections (see Appendix A). B3 shows that adjusting the scaling factor in the calculation of the I_0-corrected cross sections to the true values of the different column amounts does account for the small discrepancies with the actual column amounts used for O_3. Originally, values of 1.0×10^{20} molecules cm^{-2} were used for each O_3 cross section, and values of 1.0×10^{17} molecules cm^{-2} were used for NO_2. Clearly, for measured spectra the exact amount of scaling for each I_0 correction will vary and will be unknown. However, given the accuracy of the BrO columns retrieved in analyses B2 and B3, this should not be a significant source of error. Finally, C-type analyses show by comparison to A2 and B2 that small changes in the analysis wavelength window used can have a significant effect on the retrieved BrO if non-I_0-corrected cross sections are being used.

[14] The ability of each group to produce approximately the same values, especially for the I_0-corrected case, where agreement was almost perfect for each group, suggests that any differences between the various groups' retrieval of their own data are largely due to differences in calibration, cross sections, instrumental factors, and, in some cases, differences in the method of the analysis (e.g., Heidelberg and CNRS).

[15] The importance of using I_0-corrected cross sections is clearly illustrated in Figure 2. Figure 2a shows the fit to BrO after the removal of all other absorbers when using non-I_0-corrected cross sections (analysis B1), and Figure 2b shows the same when using I_0-corrected cross sections (analysis B3). Relatively large residual structures are left in Figure 2a that are not evident in Figure 2b. Different values for the BrO slant column difference are produced in the two different analyses (see Table 3), with the correct value being retrieved in the I_0-corrected case. As will be shown in section 6.5, the use of I_0-corrected cross sections has a significant effect on the retrieved BrO column amount when analyzing real atmospheric spectra, though the differential spectra are often too noisy to readily reveal the effect on the residual absorption. Smoothing of the spectra prior to analysis does, however, enable these changes in the residual features to be seen.

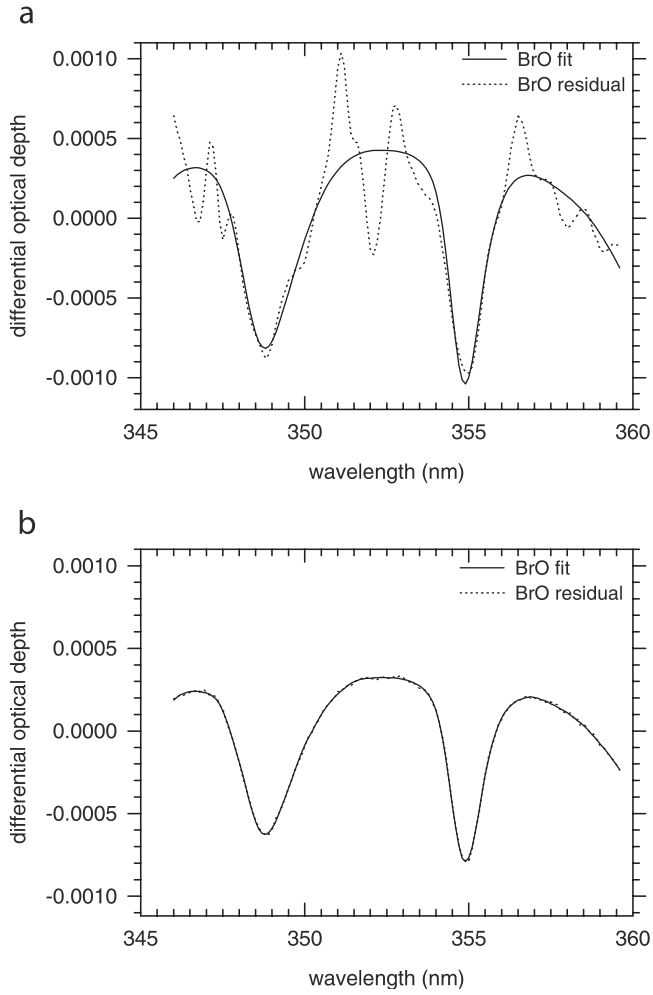

Figure 2. Bremen group fit of BrO to the optical depth after removal of absorptions due to O_3, NO_2, and O_4 in the synthetic differential spectrum, using (a) non-I_0-corrected cross sections and (b) I_0-corrected cross sections.

6. Sensitivity Studies

[16] Since there were some large discrepancies between the results of the various groups (see Figure 1), examinations of the sensitivity of the analysis to a variety of analysis parameters were carried out. Initial tests having indicated that sensitivity to the various changes may be different from group to group, the study was conducted on a representative set of data from five instruments out of the six involved in the intercomparison: Bremen, Heidelberg, IASB, NILU, and UCam, all treated with the IASB software. The data analyzed are those measured simultaneously by the five instruments, i.e., on 24–25 June and

on 26 June 1996 after noon. The NIWA spectrometer was not optimized for BrO observations during the campaign, suffering from poor transmission at 350 nm resulting in noisy results not representative of measurements usually performed by the NIWA group. Therefore data from this latter instrument were not included in this part of the study.

[17] This work largely builds upon initial sensitivity tests carried out for BrO analysis by the UCam group [e.g., *Aliwell et al.*, 1997]. The standard case used for comparison was analysis using the *Harder et al.* [1997] 227-K NO_2 cross section, the Global Ozone Monitoring Experiment (GOME) [*Burrows et al.*, 1999] O_3 cross sections (221 and 241 K) with shifts of +0.03 nm, the *Wahner et al.* [1988] BrO cross section (223 K) with a shift of +0.17 nm, and the *Greenblatt et al.* [1990] O_4 cross section (298 K) with a shift of -0.0868 nm and a stretch of 5.22×10^{-3}. A second-order polynomial was used in deriving the differential cross sections and spectra, and the fitting procedure was carried out over the wavelength region 346–359 nm. The O_3 and NO_2 cross sections were corrected for the I_0 effect. The Ring cross section was derived from rotational Raman scattering calculations according to the simplified yet accurate method described by *Chance and Spurr* [1997]. A more elaborated method treating infilling of molecular structures and atmospheric radiative transfer effects is described by *Vountas et al.* [1998]. Wavelength calibration of the measured atmospheric spectra used the Kitt Peak solar spectrum [*Kurucz et al.*, 1984], the accuracy of which is quoted to be better than 0.001 nm. Correction for a linear offset in the measured intensities was allowed in the fitting procedure.

[18] What follows is a discussion of the various sensitivity tests performed and of their significance. Results of test analyses are summarized in Figures 3a and 3b in Tables 4 and 5. In total, 14 test cases have been considered, each described in brief in Table 4, column 2. Figures 3a and 3b display, for each test case and as a function of the solar zenith angle, the percent difference in retrieved BrO differential slant columns relative to the standard case. Different symbols are used to identify the various data sets, so that instrument-related differences in sensitivity can be easily detected. Mean deviations calculated in the most commonly used range of solar zenith angles, 87°–90°, are given in Table 4. The last column represents, for each test case, the net impact of the analysis change considered, averaged on all instruments. Table 5 shows percent differences in BrO slant columns relative to values obtained with the UCam instrument (also in the range 87°–90° SZA). This gives an indication of how the various instruments may be affected differently by the changes in analysis settings. The overall agreement is quantified in a single number for each test case by calculating the standard deviation of all BrO differential slant columns retrieved between 87° and 90° SZA (last column of Table 5).

6.1. Accuracy of BrO Absorption Cross Section

[19] Systematic errors in the retrieved BrO slant columns as a result of inaccuracies in the shape and wavelength calibration of the absorption cross sections used are likely to be a significant problem. Previous work suggested that the 223-K BrO cross section of *Wahner et al.* [1988] required a shift of +0.17 nm [*Aliwell et al.*, 1997]. The direction and approximate magnitude are confirmed by comparison with Fourier transform spectrometry (FTS) measurements of the relative and absolute BrO absorption cross sections made at Harvard University [*Wilmouth et al.*, 1999] and at the University of Bremen (O. Fleischman et al., Measurements of the spectroscopy and kinetics of BrO by time-resolved Fourier transform spectroscopy, manuscript submitted to *Journal of Photochemistry and Photobiology*, 2001; data available from http://www.iup.physik.uni-bremen.de/gruppen/molspec/index.html), respectively. Although previous results indicated that relatively small shifts (on the order of 0.05 nm) do not affect the retrieved BrO slant column greatly, results from test 1 (see Table 4 and Figure 3a) show that the shift of +0.17 nm leads to a significant difference in the BrO slant column retrieved relative to the unshifted case. The difference as a result of not including the shift in BrO is a systematic overestimation of the retrieved BrO columns by 23% on average between 87° and 90° SZA (see Table 4). As can be seen, some instruments show larger sensitivity than others to the shift applied. The reason for this behavior is unclear. It is probably related to the fact that BrO and O_3 shifts are in effect not independent (see section 6.2). Note, however, that not shifting BrO results in a significant increase of the scatter between groups (see Table 5).

[20] The resolution of the *Wahner et al.* [1988] cross section is ~0.4 nm and so is somewhat too low for the resolution of the instruments taking part in this study. In smoothing the cross sections to instrument resolution, falsely high values of BrO will be recorded depending on the resolution in the range used by the instruments tested here. This effect has been investigated in test case 3, where BrO differential slant columns have been retrieved using the recent *Wilmouth et al.* [1999] BrO cross section. The resolution of this data set is 0.12 nm FWHM at 350 nm, which is sufficient to enable accurate smoothing to the various instrument resolutions. Results of test 3 given in Table 4 show that incorrect smoothing of the *Wahner et al.* [1988] BrO cross sections may account for only a few percent difference between the different groups' analyses. As expected, the smallest difference with the reference evaluation is obtained with the NILU instrument, which has the poorest resolution (0.9 nm). Note also the very good consistency between the two sets of cross sections resulting in almost identical BrO values when smoothed at this low resolution.

6.2. Accuracy of O_3 Absorption Cross Sections

[21] The BrO analysis was previously found to be quite sensitive to the wavelength calibration of the O_3 cross sections when fitting over the 345- to 360-nm wavelength range [*Aliwell et al.*, 1997]. In that case, using non-I_0-corrected cross sections over the 345- to 360-nm range, the unshifted analysis was found to give BrO values some 28% higher than the correct shifted analysis. Repeating the test using the standard conditions specified above (i.e., 346–359 nm and I_0-corrected cross sections) shows a reduced sensitivity to shift of some 5% on average between

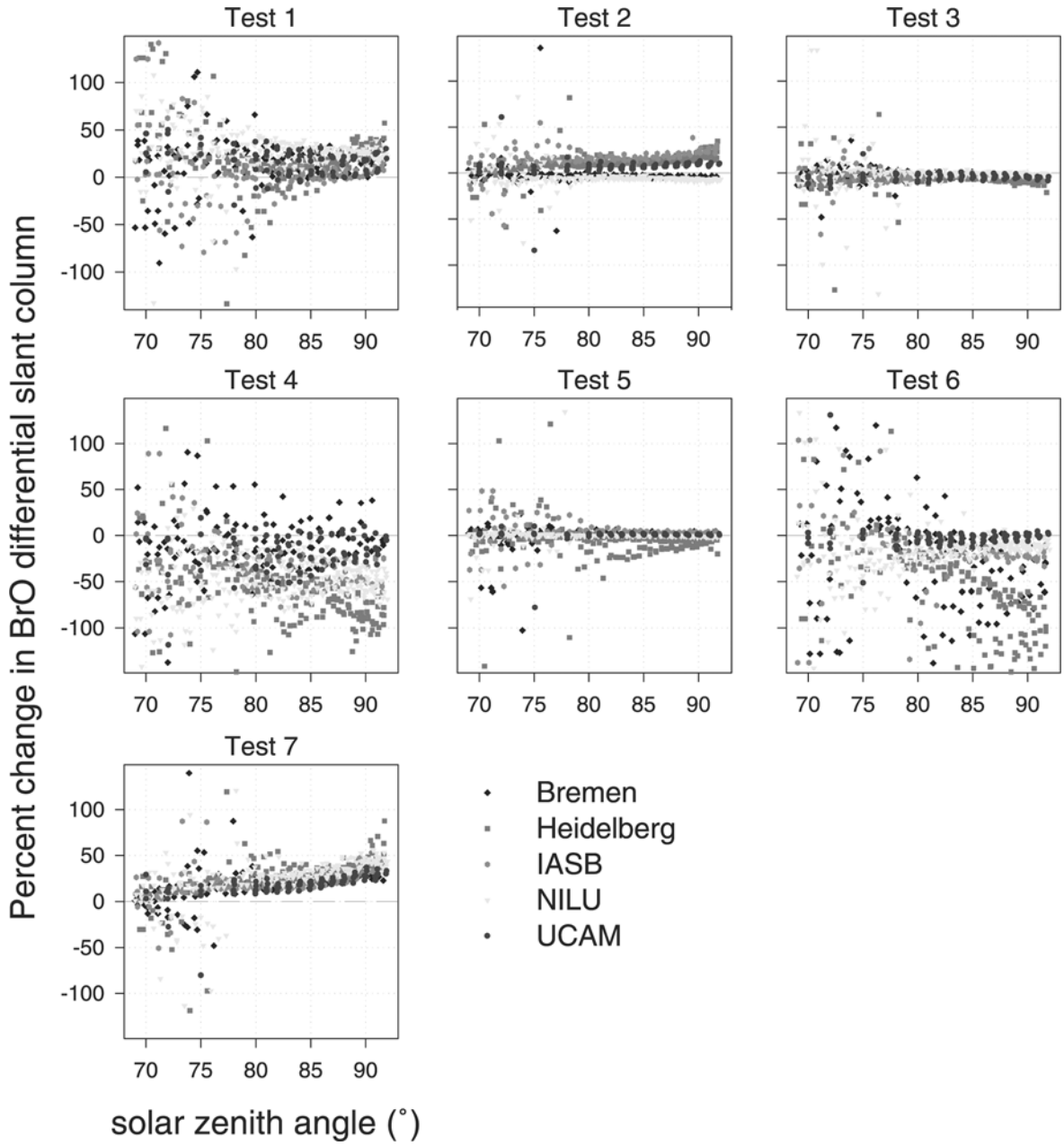

Figure 3. Results from sensitivity tests (a) 1–7 and (b) 8–14. Percent changes in BrO differential slant column relative to the standard evaluation are displayed as a function of the solar zenith angle using different colors for each instrument. A brief description of the nature of each test can be found in Table 5 or 6.

87° and 90° SZA but, again, with significant differences when looking at individual instruments (see results from test 2). Note that instruments showing large dependence to O_3 shift (e.g., IASB) generally show comparatively smaller dependence to BrO shift, which suggests that the two effects may not be independent. Note also in Table 5 that the similar increase in the scatter of BrO results for test cases 1 and 2.

[22] Previous work [*Aliwell et al.*, 1997] had suggested that a shift of +0.02 nm in the calibration of the GOME O_3 cross sections was appropriate when analyzing spectra measured at Aberdeen, Scotland, during the winter of 1994/1995. This shift was derived from attempts to minimize the residual of the fit. Work during this intercomparison has shown that for the measurements made at OHP, a shift of approximately +0.03 nm was most appropriate based on minimizing the residual of the fit. FTS measurements of the O_3 cross sections by the Bremen group [*Voigt et al.*, 2001] have since confirmed that a +0.03-nm shift of the GOME O_3 cross sections is required. This shift is within the known accuracy of the wavelength calibration of the GOME flight-model instrument made during the preflight measurements of the O_3 cross sections [*Burrows et al.*, 1999]. The reasons for the different shifts

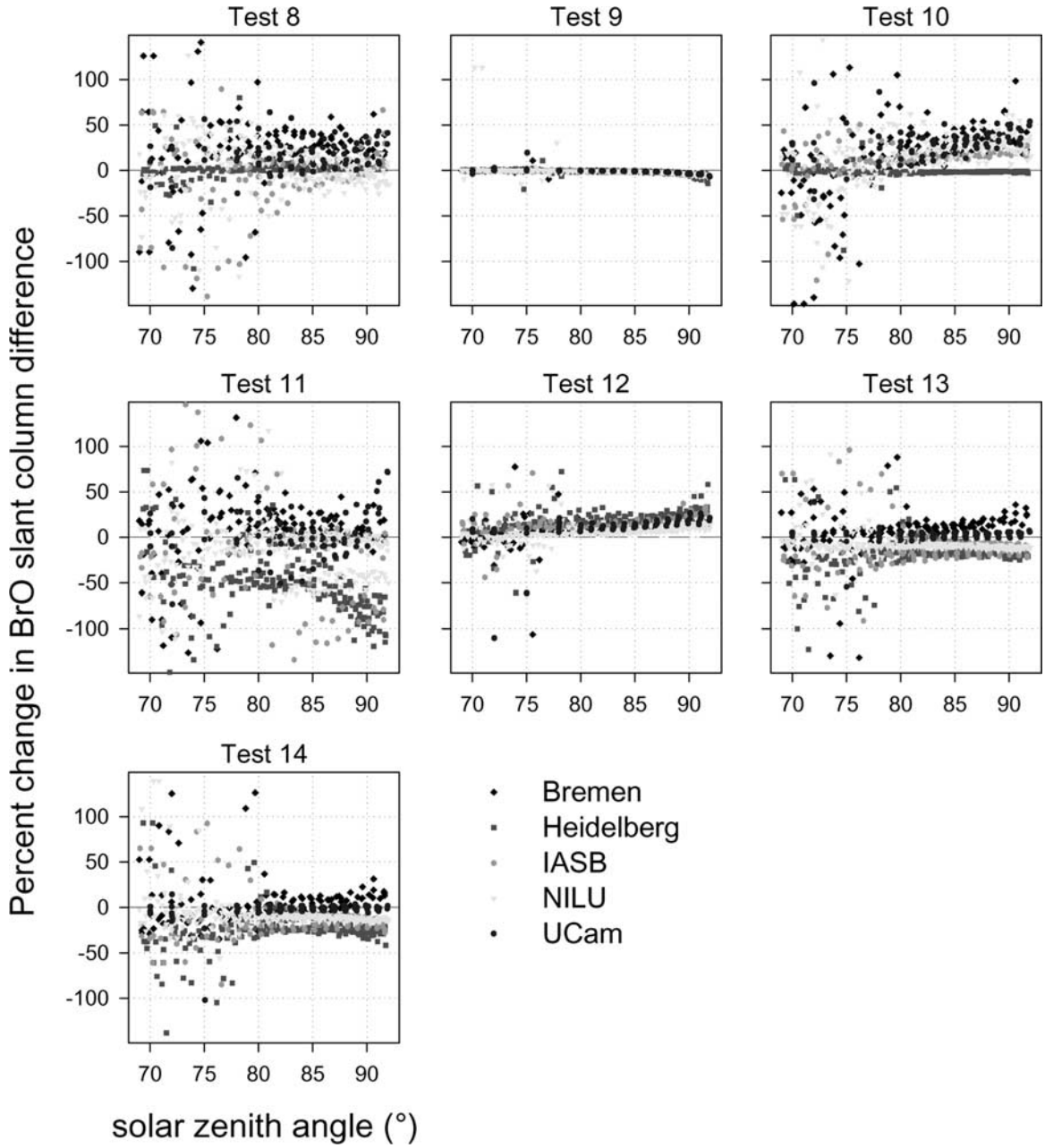

Figure 3. (continued)

for the analysis of the Aberdeen and OHP data are not clearly understood at present. They are probably at least partially the result of nonlinearities in the O_3 cross-section temperature dependence, which would affect the proportions of each of the two O_3 cross sections fitted when the atmospheric temperatures are so different.

6.3. Temperature Dependence of O_3 Absorption Cross Sections

[23] Since the O_3 cross section has a strong temperature dependence in the UV [e.g., *Brion et al.*, 1993], it was previously suggested that two different temperature cross sections fitted simultaneously be used in order to account for the effect of having O_3 at different temperatures in the stratosphere. The cross sections chosen were at 221 and 241 K, which should be approximately representative of stratospheric temperatures. Although it has proven to be useful in practice, the method of fitting two cross sections in order to describe O_3 at different temperatures is clearly an approximation that, to correctly describe a temperature profile, would require the temperature dependence of the cross sections to be linear. As mentioned earlier, nonlinearities in the temperature dependence may be the origin of some unanswered problems such as, for example, the different O_3 cross-section shifts derived from Aberdeen and OHP data (see section 6.2). The impact of not accounting for the temperature dependence has been investigated in test case 10, where BrO was retrieved with one O_3 cross section (241 K) instead of two. Results shown in Figure 3b and Table 4 indicate a strong and

Table 4. Summary of BrO Retrieval Sensitivity Tests Carried Out Using the DOAS Software From IASB Applied to Spectra From Bremen, Heidelberg, IASB, NILU, and UCam Instruments[a]

Test	Test Description	Bremen	Heid	IASB	NILU	UCam	Mean
1	BrO cross section [*Wahner et al.*, 1988], not shifted	16	26	4	31	15	23
2	O_3 cross sections (GOME 221 and 241 K), not shifted	−4	15	21	−9	9	5
3	BrO cross section [*Wilmouth et al.*, 1999]	−4	−8	−4	−1.1	−4	−4
4	fitting interval: 345–360 nm	0.9	−78	−36	−31	−7	−40
5	fitting interval: 346–360 nm	0.8	−6	4	−0.8	0.6	−1.6
6	fitting interval: 346–365 nm	−38	−82	−23	−5	−0.9	−34
7	no I_0 correction	26	33	26	47	24	35
8	polynomial of degree 3	29	1.3	4	4	24	8
9	wavelength-dependent air mass factor corrected	−3	−4	−2	−4	−3	−3
10	fit only one O_3 cross section (241 K)	37	−1.6	17	45	34	25
11	no offset correction	9	−78	−27	9	14	21
12	shift spectra by −0.01 nm relative to all cross sections	15	21	20	13	17	17
13	slit function determined by DOAS algorithm	17	−18	−15	−13	3	9
14	same as test 13, but using *Wilmouth et al.* [1999] BrO cross section	9	−26	−18	−14	−0.9	−14

[a]Numbers give, for each test case, the percent change in BrO slant column difference relative to the standard analysis, averaged in the solar zenith angle range 87°–90°.

consistent impact for all tested instruments except the Heidelberg instrument. On average for the OHP conditions, the effect of not accounting for the O_3 cross-section temperature dependence is an overestimation of the BrO slant columns by 25% between 87° and 90° SZA.

6.4. Selection of the Wavelength Interval

[24] The selection of the wavelength interval over which the analysis is to be carried out was found to be a significant source of systematic differences in the BrO slant column retrieved. This has been investigated for a selection of wavelength intervals considered in test cases 4, 5, and 6. We see that even small adjustments to the width of the analysis window can cause significant differences in the retrieved BrO slant columns. This is probably indicative (at least partially) of the effects of interference by correlating and/or poorly fitting other absorbers. By shortening the interval, it is possible to exclude some absorption features that would otherwise interfere with the quality of the fit; however, at the same time, the degree of correlation of the cross sections fitted is increased. We also see that the sensitivity to changes in the width and position of the fitting interval varies significantly from instrument to instrument (compare, for example, the results obtained for UCam and Heidelberg). This large instrument-dependent variability in sensitivity leads to increased scatter of BrO results as seen in Table 5, especially for test case 6. Such a behavior points to the role of instrumental effects that may differently interfere with the quality of the BrO fit, depending on the wavelength region considered for the fit. In the cases investigated here the analysis is less sensitive to small changes on the long-wavelength side of the interval than to similar changes on the short-wavelength side where O_3 differential structure is largest. The largest change is seen when extending the interval from 346 to 345 nm. Clearly, the selection of a suitable wavelength region that minimizes interference from poorly characterized ''absorption'' features but nevertheless allows sufficient wavelength range

Table 5. Summary of BrO Retrieval Sensitivity Tests Carried Out Using the DOAS Software From IASB[a]

		Percent Difference in BrO Slant Column Relative to UCam				BrO SD
Test	Test Description	Bremen	Heidelberg	IASB	NILU	($\times 10^{13}$ molecules cm^{-2})
0	standard analysis	−17	26	17	18	3.4
1	BrO cross section [*Wahner et al.*, 1988], not shifted	−16	39	8	31	4.9
2	O_3 cross-sections (GOME 221K & 241K), not shifted	−26	32	30	1.6	4.3
3	BrO cross-section [*Wilmouth et al.*, 1999]	−17	21	17	22	3.1
4	fitting interval: 345–360 nm	−10	−71	−18	−29	4.2
5	fitting interval: 346–360 nm	−16	15	20	16	3.3
6	fitting interval: 346–365 nm	−62	−92	−9	6	7.4
7	no I_0 correction	−15	35	18	31	4.6
8	polynomial of degree 3	−12	8	0.2	−2	2.9
9	wavelength-dependent air mass factor corrected	−17	24	17	17	3.3
10	fit only one O_3 cross section (241 K)	−15	−8	1.9	14	3.7
11	no offset correction	−11	−67	−29	−10	5.6
12	shift spectra by −0.01 nm relative to all cross sections	−18	30	19	12	4.0
13	slit function determined by DOAS algorithm	−5	3	−0.8	2	2.7
14	same as test 13, but using *Wilmouth et. al* [1999] BrO cross section	−7	−4	0.1	5	2.5

[a]Applied to spectra from Bremen, Heidelberg, IASB, NILU, and UCam instruments. Table shows the evolution of the overall agreement between instruments for the different test cases considered. Percent difference in BrO slant columns relative to UCam results, and standard deviations of BrO slant columns (all groups together), are calculated in the solar zenith angle range 87°–90°.

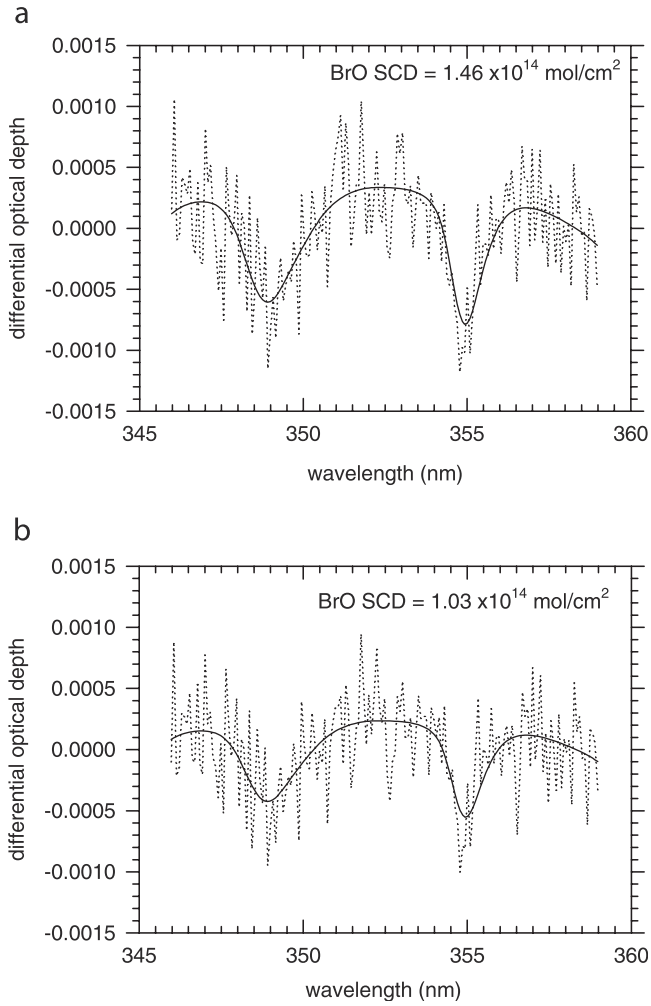

Figure 4. Bremen group fit of BrO to the optical depth after removal of the absorptions due to O_3, NO_2, O_4, Ring, and Rayleigh using (a) non-I_0-corrected cross sections and (b) I_0-corrected cross sections.

coverage to give a good degree of noncorrelation between the cross sections is of paramount importance.

6.5. Impact of Correcting Absorption Cross Section for the I_0 Effect

[25] The use of cross sections corrected for the solar I_0 effect has already been mentioned in section 5 (see also Appendix A). Test case 7 shows the effect of not using I_0-corrected O_3 cross sections in the analysis of real atmospheric spectra. The difference made by not using the I_0-corrected cross sections is consistently found by each instrument to be significant and variable with SZA. Between 87° and 90° SZA the effect of not using the I_0-corrected cross sections is to overestimate the BrO slant column by 35% on average (see Table 4 and Figure 3a). The dependence on the SZA is likely due to the fact that O_3 makes a larger contribution to the total differential absorption at large SZA than at small SZA (the O_3 slant column increases faster as a function of SZA than the BrO slant column), so the impact of the I_0 correction is expected to be larger at large SZA. As mentioned in section 5, while the use of the I_0-corrected cross sections makes a significant difference to the amount of BrO retrieved, improvements to the residual of the fit are not as readily visible as was the case with the synthetic spectra. Figure 4a shows the fit of the BrO cross section to the differential optical depth remaining after the removal of all other absorption features has been attempted using non-I_0-corrected cross sections. Figure 4b shows the fit where I_0-corrected O_3 cross sections have been used. Note the reduction by ~30% in the BrO slant column compared to results from Figure 4a. Clearly, the differential spectra are very noisy, especially when compared to previous observations at higher-latitude sites in winter [e.g., *Aliwell et al.*, 1997; *Eisinger et al.*, 1997; *Otten et al.*, 1998]. This noise may have a variety of sources, including large interpolation errors due to larger temperature-dependent shifts of the wavelength registration or unaccounted for variability in the sensitivities of the various detector pixels to the signal measured. In the case of CCD detectors this interpixel variability effect is measured and accounted for. Diode array detectors exhibit this effect to a far smaller degree, so such corrections are not generally made. It is possible that at the detection levels required for BrO analysis, such effects are significant and have not been sufficiently well accounted for. It should be noted that the O_3 concentration in the synthetic spectra is approximately similar to those seen in measured spectra, so a smaller contribution of the I_0 effect is not likely. Some of the spectral features due to the use of non-I_0-corrected cross sections are expected to be of comparable amplitude to the spectral noise, so unlike the case of the noise-free synthetic spectra, these may be masked to some extent. In the analysis employed by NIWA the spectra are filtered prior to the analysis to remove some of the higher-frequency noise, and the improvement in the residual is clearly visible, with features similar to those seen in the synthetic case being evident. These differential fits for the uncorrected and corrected cases are shown in Figures 5a and 5b. It should be noted (see Appendix A) that this correction is not necessary where cross sections are measured using the zenith-sky instrument and a cell with the zenith sky as the light source (e.g., National Oceanic and Atmospheric Administration group).

6.6. Role of the Polynomial Order

[26] There is some sensitivity to the degree of the polynomial used in the fit and generation of the differential cross sections. This is illustrated in test case 8, where a polynomial of third order has been used instead of the second-order polynomial applied in the reference analysis. As mentioned in section 5, the role of the polynomial is to account for the unstructured part of the differential optical thickness (a complex combination of Rayleigh, Mie, and (residual) broadband attenuation terms). The approximation of a low-order polynomial is justified by the small width of the BrO fitting interval. Increasing the degree of the polynomial may account for larger curvatures, but at the expense of a reduction in the number of degrees of freedom of the problem and hence at a reduced precision. The relatively small sensitivity found in test 8 (8% change in BrO slant column on average) suggests that the choice of a second-order polynomial is in general close to an optimum for the selected BrO interval.

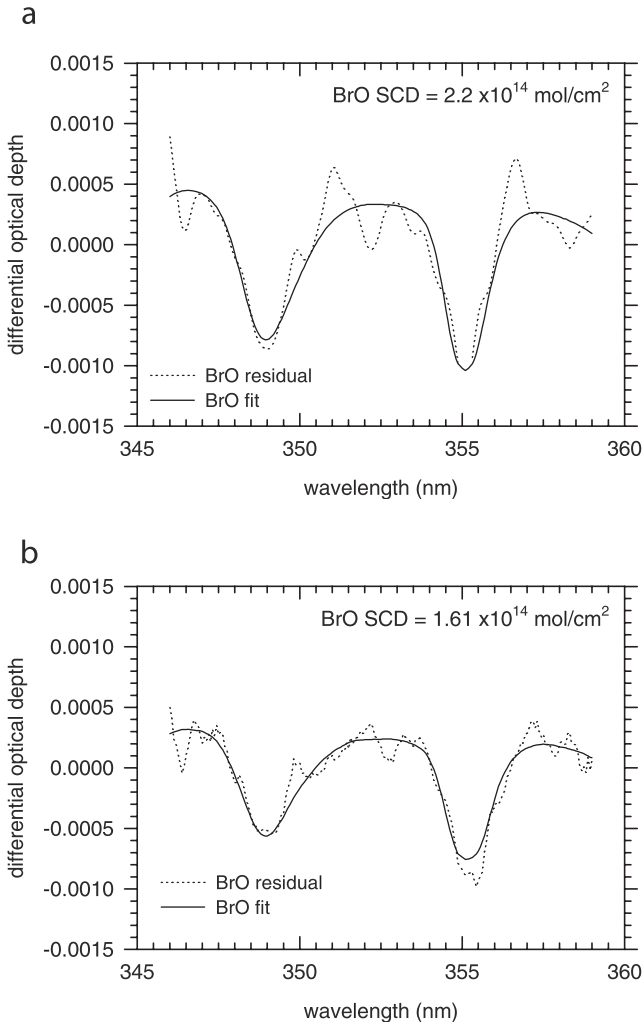

Figure 5. NIWA group fit of BrO to the filtered optical depth after removal of the absorptions due to O_3, NO_2, O_4, Ring, and Rayleigh using (a) non-I_0-corrected cross sections and (b) I_0-corrected cross sections. In contrast to Figure 4, these spectral data are smoothed.

Note, however, that some groups' results (see, e.g., Bremen) are more sensitive to the choice of the polynomial order than others. The fact that the overall scatter of results is reduced when using a third-order polynomial (see test case 8 in Table 5) suggests that for these instruments, correction for greater curvature would be needed.

6.7. Wavelength Dependency of O_3 Air Mass Factors

[27] The analysis was also tested for its sensitivity to the use of wavelength-dependent air mass factor (AMF) corrections to the O_3 cross sections. Basically, what happens is that because the atmosphere is not optically thin in this part of the UV, due to strong absorptions by O_3, the average altitude from which comes the majority of light scattered down into the spectrometer varies according to the O_3 absorption cross section. At wavelengths where there is a strong absorption band the average scattering altitude is pushed down since most light from above has been absorbed. This effect has also been described as an optical path length filtering process [*Marquard et al.*, 2000]. Accordingly, the O_3 cross sections need to be corrected for by multiplying by wavelength-dependent air mass factors as calculated using a scattering model [e.g., *Fish et al.*, 1995]. These are then fitted in place of the actual cross sections and effectively fit the vertical column amount. Such corrected cross sections were calculated here using the UVSPEC software package (A. Kylling, UVSPEC: A program package for calculation of diffuse and direct UV and visible intensities and fluxes, available by anonymous ftp to kaja.gi.alaska.edu, cd pub/arve, 1995), which implements the pseudospherical radiative transfer model DISORT [*Dahlback and Stamnes*, 1991]. Air mass factor calculations included multiple scattering for a model atmosphere including O_3 as well as Rayleigh and aerosol scattering. The temperature, pressure, and O_3 vertical profiles used in the calculation were obtained from sonde measurements made in support of this campaign at Gap (80 km from OHP) on the same day. The results of using the AMF-corrected cross sections are shown in Table 4 and Figure 3b (test case 9). The corrected analysis gives BrO values slightly smaller than the standard analysis, but the difference is definitely small. Between 87° and 90° SZA the AMF-corrected analysis is 3% less than the standard analysis. Given the other sources of error, however, this correction does not appear to be a significant improvement on the standard analysis. Previous work using this correction [*Fish et al.*, 1995; *Richter et al.*, 1999] had shown greater improvements to the residual of the fit and significant changes to the amount of BrO fit. This was, however, prior to the use of two O_3 cross sections to account for the temperature dependence effect. The improvements due to the AMF-corrected cross sections came largely from the treatment of O_3 temperature dependence in the radiative transfer model used in their calculation.

6.8. Offset Correction

[28] An ideal spectrometer operated in an ideal atmosphere would measure that part of the sunlight that has been elastically scattered by air molecules and particles in the zenith direction. In a real experiment, however, a number of possible additional sources of signal may add to the ideal Rayleigh/Mie contribution, causing an "offset" to the measured intensity. To a first approximation, the Ring effect, which is mainly due to inelastic Raman scattering by O_2 and N_2 molecules [e.g., *Solomon et al.*, 1987], is a natural source of offset that has received much attention in the data analysis. In addition to the Ring effect, instrumental sources of offset also need to be considered, such as stray light in the spectrometer or imperfectly corrected dark current of the detector. The accurate characterization of these instrumental effects (especially stray light) often proves to be difficult in the field, hence most analysis packages include the possibility of fitting an offset parameter. Note that because of a cancellation effect when taking the ratio of spectra, the analysis can only correct for a difference in the offsets possibly present in both spectrum and reference. A large offset that is present at the same level in both spectra would therefore not be detected even though it directly affects the accuracy of the retrieval. The reference evaluation in this study used a linear offset correction for all instruments. In test case 11 the impact of not including this

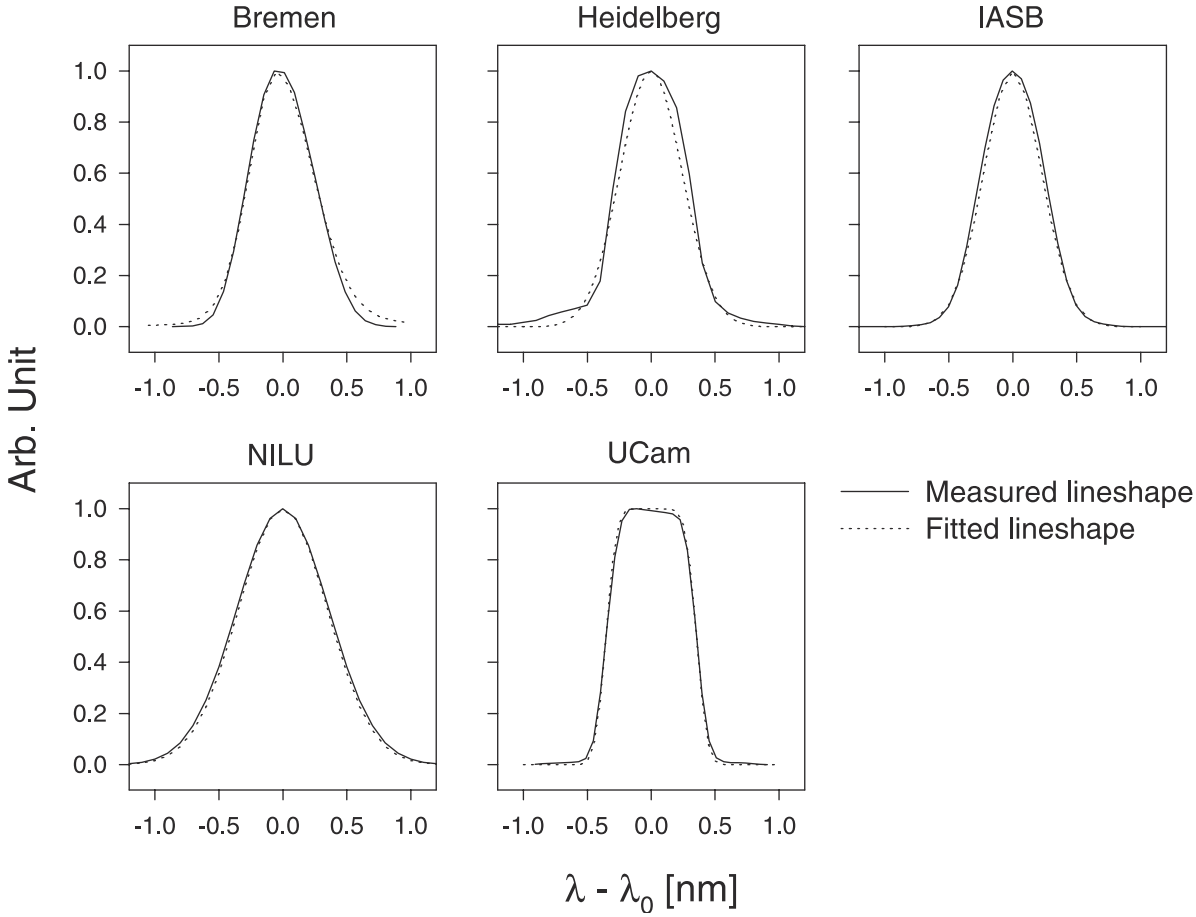

Figure 6. Slit functions for Bremen, Heidelberg, IASB, NILU, and UCam instruments, as measured in the laboratory (solid line) and as determined using the IASB fitting algorithm (dotted line).

correction was investigated. Results in Figure 3b and Table 4 show quite clearly that the magnitude of offset effects is strongly instrument dependent. We see, for example, a rather small impact in the case of Bremen and NILU data, while the Heidelberg instrument requires a much larger correction. Evidence for poor scattered light rejection is also found when looking at the shape of the measured slit function of the Heidelberg instrument, which appears to have a signal that extends very large lambda-lambda nought values (see Figure 6). This points to the importance of careful instrument design and characterization in minimizing instrumental sources of offset.

6.9. Accuracy of the Wavelength Calibration of Measured Spectra

[29] As mentioned in section 6.2, it was found that a shift of +0.03 nm of the GOME O_3 cross sections [*Burrows et al.*, 1999] could be used to minimize the residual of the fit. However, if all the cross sections are then subject to further shifts simultaneously, the residual is sometimes found to reduce further. The minimum residual is clearly found after further simultaneous shift of all cross sections. This is in effect equivalent to a change in the wavelength calibration of the measured spectrum. For other spectra and on other days this shift was often either not necessary or was even in the opposite direction. A similar behavior is found by other groups when analyzing their own data.

[30] The accuracy of the wavelength calibration of measured spectra is a key issue because it determines how well measured spectra can be aligned with laboratory cross sections. Initial tests in this study have confirmed that excellent precision can be obtained by correlating measured atmospheric spectra with the Kitt Peak solar atlas [*Kurucz et al.*, 1984]. The above results suggest, however, that there may still be a problem with the absolute wavelength calibration of the analyzed spectra, in addition to the already recognized shifts to the cross sections required. It is, in fact, likely that the wavelength calibration and resolution of the Fraunhofer spectrum used for the calibration is insufficient to fix the spectral calibration to much better than a hundredth of a nanometer, as would be required to match the size of the necessary shifts in the cross sections that cause such significant differences to BrO retrieval. The impact on the BrO slant columns of an uncertainty on the order of 0.01 nm on the calibration of spectra was checked in test case 12. Clearly, all instruments show a similar sensitivity to this error source (18% on average between 87° and 90° SZA for a shift of 0.01 nm).

6.10. Role of the Instrument Slit Function

[31] A further limiting factor on the accuracy of the spectral evaluation is the correctness of the measured slit function in each case. A poorly representative slit function

may be caused by measurement of a line source at an unsuitable wavelength or by incorrect filling of the instruments' field of view when measuring the line source. Such inadequacies in the slit function will affect both the calibration of the spectra and the smoothing of the cross sections to match the absorption shapes in the differential spectra. The slit function has been shown to be sensitive to wavelength and temperature, depending upon the characteristics of the individual instrument. In order to try and help minimize these problems, an alternative technique for determining the slit function using the Fraunhofer features in the actual measured spectrum has been developed and implemented in the IASB analysis package. The technique consists of a nonlinear least squares procedure where a measured spectrum is fitted to a high-resolution solar atlas [*Kurucz et al.*, 1984] degraded to the spectrometer resolution using a parameterized slit function that is adjusted as part of the least squares fit. Although limited in its accuracy by the need to use existing analytic functions to represent the various instrumental line shapes, the method is easily applicable and allows possible wavelength dependencies of instrumental slit functions to be identified. Figure 6 shows a comparison of the slit functions of the instrument tested here, as measured by each group (solid line) and as determined by the IASB algorithm (dotted line). Small but significant wavelength dependences (not shown in Figure 6) have been identified and considered for the Heidelberg instrument. These results have been used in test case 13 to investigate the impact of changing slit functions on the BrO retrieval. For this test case the calibration of the spectra and the smoothing of the cross sections were performed using the slit functions determined using the IASB algorithm. Results given in Table 4, showing differences in retrieved BrO slant columns ranging from 3 to 18%, confirm that the uncertainty on the slit function is likely to play a significant role in explaining the differences between groups. This is further confirmed by the analysis displayed in Table 5, which shows that the consistency between instruments is significantly improved for test case 13 compared to the standard analysis. As can be seen, the net effect of test case 13 is to decrease the values from Heidelberg, IASB, and NILU and to increase Bremen values so that better matching is obtained with UCam (results from this latter group being practically unchanged). The best overall agreement (<10% difference between each set of results) is finally obtained for test case 14, which is similar to case 13 except that BrO cross sections are from *Wilmouth et al.* [1999] (correctly smoothed to instrument resolutions) instead of *Wahner et al.* [1988].

6.11. False BrO Signatures

[32] An important test of the sensitivity of the analysis is the possibility of detecting false amounts of BrO in the absence of BrO. In order to test this effect, synthetic spectra were produced with no BrO contribution. The result is that applying the standard analysis with I_0-corrected cross sections leads to very small negative BrO slant columns (on the order of -5.0×10^{11} molecules cm^{-2}). This confirms that the analysis algorithm is able to detect the absence of BrO to a reasonable degree. When non-I_0-corrected cross sections were used, a positive slant column of 5.0×10^{13} molecules cm^{-2} was detected, which is of the order of the errors in the synthetic data tests discussed in section 5. However, the quality of the erroneous fit is poor and would not in practice have been mistaken for the detection of atmospheric BrO. The use of I_0-corrected cross sections should therefore avoid any false detection of BrO.

7. Other Analysis Considerations

[33] OClO was not included in the fit. This is different from the case for some higher-latitude winter studies where OClO was present and therefore was analyzed for. In these summer measurements the fitting of OClO tended to produce lower residuals by fitting to features like the O_3 temperature dependence, thus affecting these fits and giving false negative amounts of OClO.

[34] The O_4 cross section of *Greenblatt et al.* [1990] measured at 298 K was used, with each group finding their own optimum shift and stretch due to differing definitions of how each group carried out spectral stretching within a particular wavelength region. This shift and stretch was necessary because the *Greenblatt et al.* [1990] measurements were made at a pressure of 55 atm and more recent measurements have shown that at atmospheric pressures the line shapes are slightly different [*Hermans et al.*, 2001]. The cross section of *Greenblatt et al.* [1990] has recently been corrected in the UV region (J. B. Burkholder, private communication, 1996). In the corrected version the bands at 342 and 380 nm have been shifted by 0.38 nm, and the band at 360 nm has been shifted by 0.84 nm. Recent measured cross sections of O_4 in the UV match well with this corrected cross section [*Hermans et al.*, 2001]. The corrected cross section and the *Hermans et al.* [2001] cross sections have not been used in the present study but are recommended for future use.

[35] The high-resolution NO_2 cross section of *Harder et al.* [1997] measured at 227 K was used. This cross section was used down to wavelengths shorter than the 350-nm published minimum wavelength, so the signal-to-noise ratio below this wavelength is relatively poor. The wavelength calibration of this cross section is expected to be very accurate, especially with respect to the Kitt Peak solar Fraunhofer spectrum. The low temperature was chosen to be approximately representative of the stratosphere. The use of more than one NO_2 cross section to describe any temperature dependence was not found to improve the analysis noticeably. This is most likely due to the low temperature dependence of the NO_2 cross section in this wavelength region. Additionally, it is necessary to keep the number of fitted variables to a minimum since, with the narrow wavelength range and the number of other fitted variables, the analysis may approach the limit of simultaneous equations relative to number of unknowns; that is, it eventually ceases to be an overdetermined solution. Thus a second NO_2 cross section would have added another parameter to be fitted for minimal return in analysis improvement.

[36] Spectra were analyzed in the SZA range from 70° to 91°. This includes the SZA of 90° that is generally reported when publishing daily values for seasonal studies. Above this SZA, spectra were often felt to be too noisy for accurate analysis. Significant divergence between the BrO slant column differences of the various groups was observed at

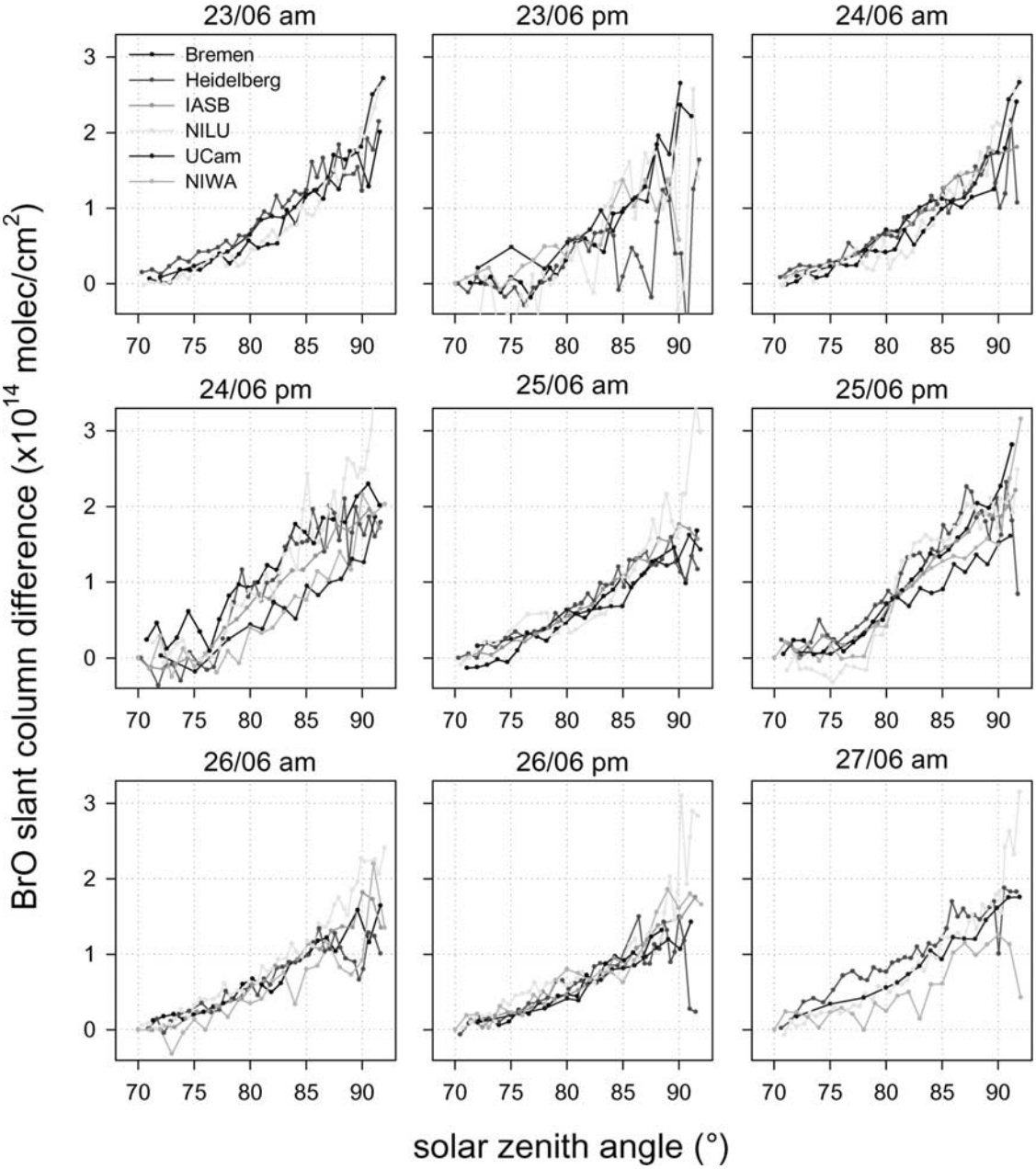

Figure 7. Comparison of BrO differential slant columns (90°–70° SZA) measured at OHP between 23 and 27 June 1996. Data are analyzed independently by each group using the constrained set of analysis parameters defined in the study (see text).

greater than ~92° SZA, probably as a result of this variation in spectral quality.

8. Recommended Analysis

[37] This study has shown that it is necessary to be very careful in the selection of the analysis parameters when attempting to fit BrO in the 345- to 360-nm wavelength region. Hence a recommended analysis at this stage with the available cross sections and other reference data is given below. This analysis has been adopted by the participating groups in the interest of uniformity of analysis, though further improvements are underway as, for example, improved absorption cross sections become available.

[38] It is recommended that for the BrO analysis the wavelength range of the fit should be 346–359 nm. Note that fitting results are by far more sensitive to changes on the short-wavelength side of the interval than on the longer-wavelength side. Measured spectra should be calibrated in wavelength by correlation to the Kitt Peak solar atlas [*Kurucz et al.*, 1984]. The O_4 cross section of *Greenblatt et al.* [1990], after suitable shift and stretch, should be used along with the recent *Wilmouth et al.* [1999] BrO cross section or the cross section by *Wahner et al.* [1988] with a shift of +0.17 nm. A suitable NO_2 cross

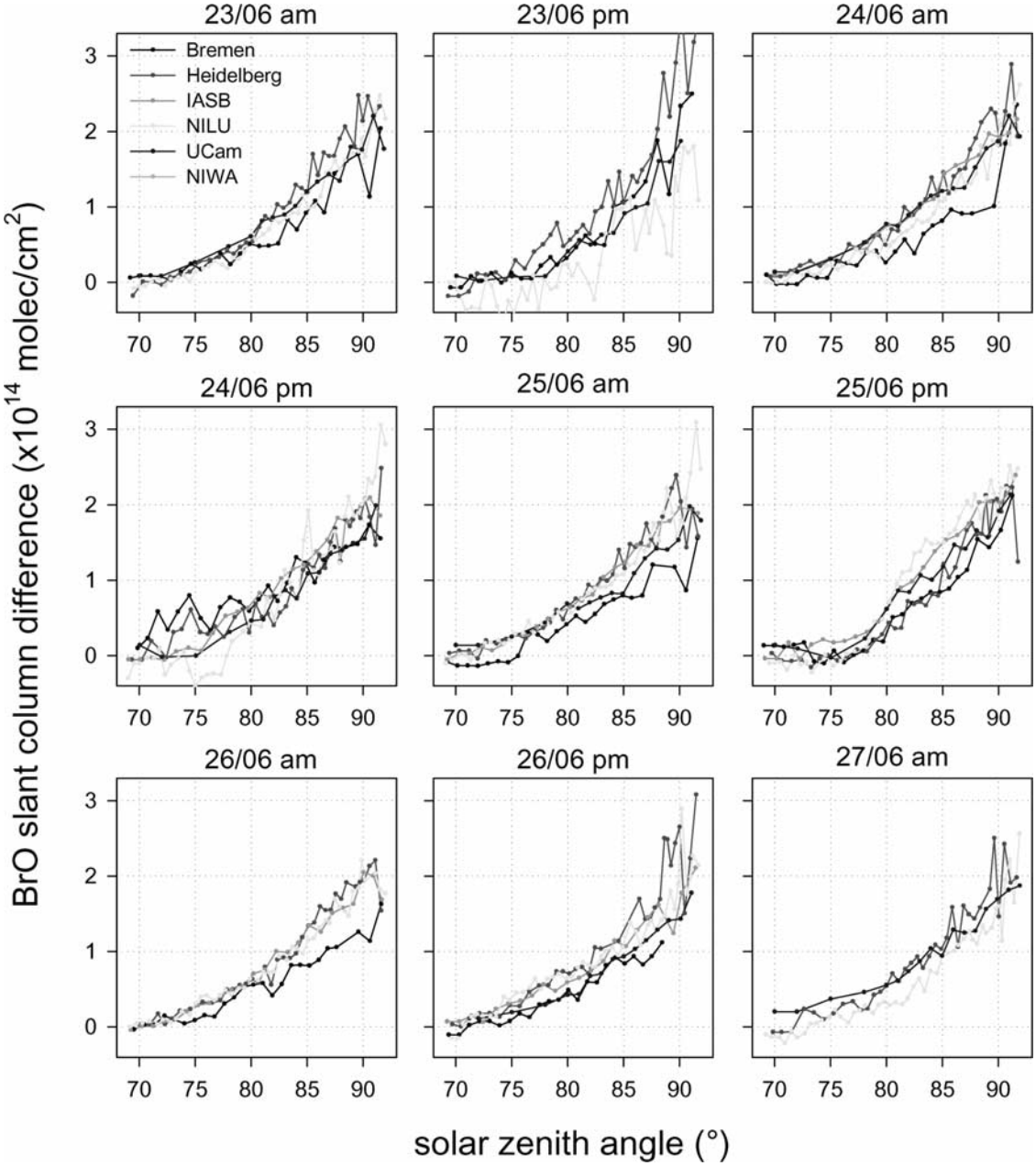

Figure 8. Comparison of BrO differential slant columns (90°–70° SZA) measured at OHP between 23 and 27 June 1996 by five out of the six participating groups. Data are analyzed by IASB using the same set of analysis parameters as in Figure 7.

section, used in the present study, is the 227-K cross section of *Harder et al.* [1997], because of its accurate wavelength calibration. However, the poor signal-to-noise ratio below 350 nm of this cross section is a drawback. It may therefore be worth considering the use of the more recent set of high-resolution (2 cm^{-1}) and high-precision wavelength calibration NO_2 cross sections measured using FTS by *Van Daele et al.* [1998]. These cover the wavelength range 240–1000 nm and have been measured at 220 K and at room temperature. The GOME O_3 cross sections at 221 and 241 K [*Burrows et al.*, 1999] should be fitted simultaneously so as to account for the temperature dependence of the O_3 cross section, but both should be shifted by +0.03 nm. The correction of cross sections for the so-called I_0 effect should be applied where laboratory-measured cross sections are used. For higher-latitude studies, especially during the winter months, OClO should be included in the fit as well.

9. Intercomparison of Results

[39] Comparisons of the analyzed BrO for each group when using the constrained set of analysis parameters are given in Figure 7. These plots include all twilight periods covered by the exercise to show the range of agreement obtained. In this and the following plots, when a particular

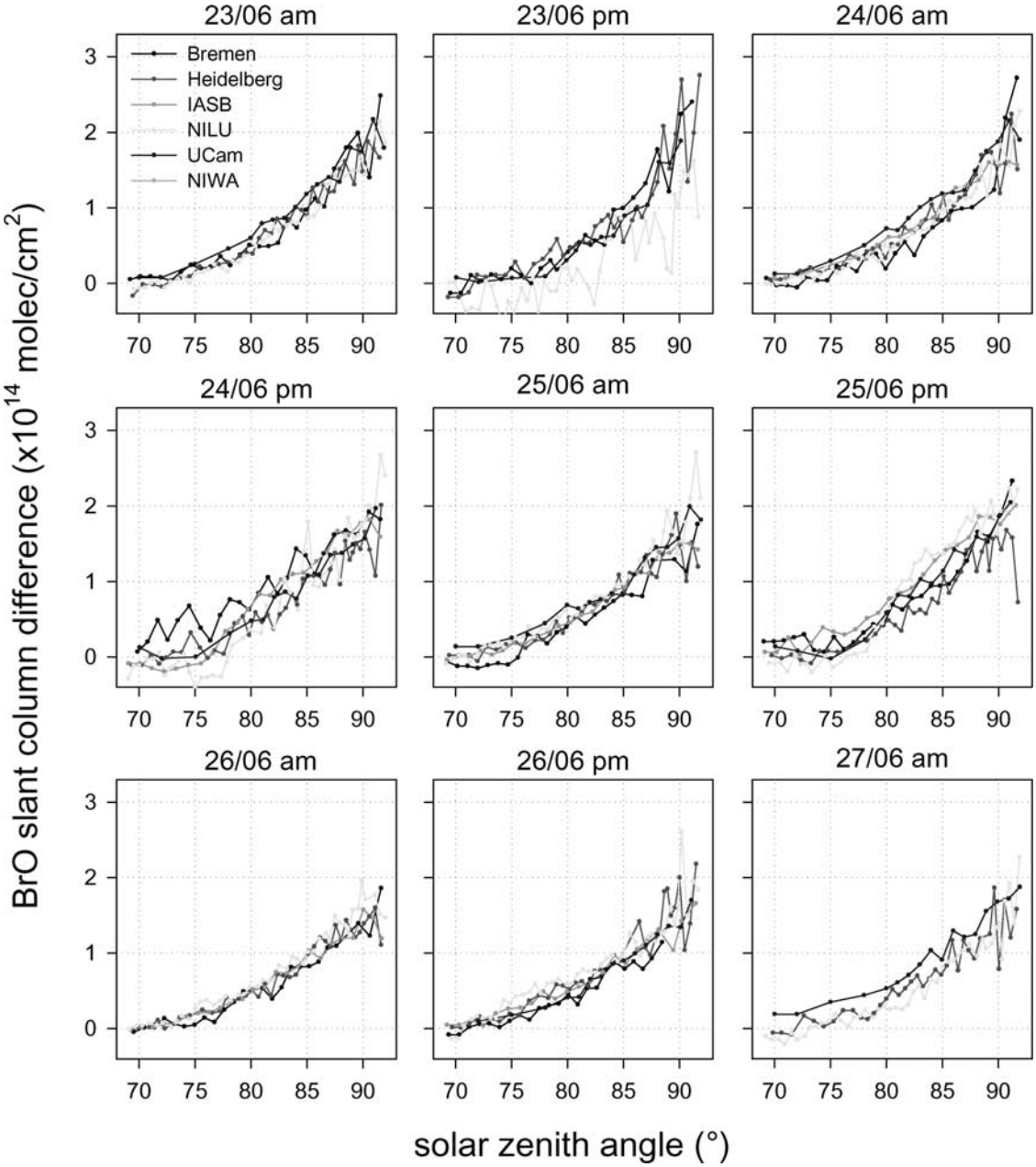

Figure 9. Same as Figure 8, but showing results from test case 14 where fitted slit functions are used instead of measured ones (see text).

group is not displayed this is due to no data having been recorded for that particular twilight period. As can be seen, the agreement between the results is greatly improved compared to initial comparison results (compare Figure 1), which suggests that the most significant causes of discrepancy have effectively been identified and minimized through this study.

[40] For comparison purposes, Figure 8 shows the results of the standard case produced with the IASB analysis package described in section 6. This analysis was performed using the same constrained analysis settings and cross sections, except for the Ring effect where a Raman calculation was used in all analysis. In contrast, in the individual groups' analysis shown in Figure 7, each group was allowed to use their own preferred method of generating a cross section to describe the Ring effect. Methods used included that of *Solomon et al.* [1987] using cross-polarization measurements and the calculation of a Ring cross section by simulation of rotational Raman scattering [e.g., *Fish and Jones*, 1995; *Vountas et al.*, 1998; *Bussemer*, 1993; *Chance and Spurr*, 1997]. After careful examination of the plots in Figures 7 and 8, one can see that in the IASB analyzed comparison the scatter of data is somewhat reduced compared to the individual analysis, despite the fact that both analyses used the same cross sections. Further reduction of the scatter is finally obtained in Figure 9, where results from the optimal IASB analysis using fitted slit functions (test case 14) are displayed. The overall level of agreement

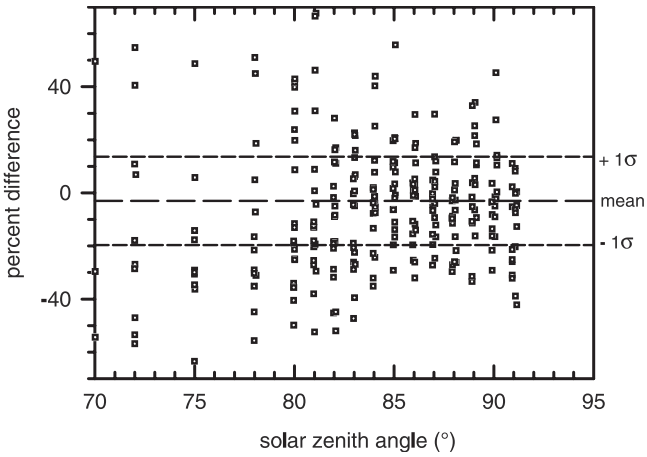

Figure 10. Fractional differences in BrO slant columns for all groups' data relative to UCam, as retrieved using the IASB analysis software and settings from test case 14. Reference lines showing the mean deviation and its positive and negative 1σ standard deviation are calculated between 87° and 90° of solar zenith angle.

obtained in this latter case is illustrated in Figure 10, where the fractional differences in BrO slant column, relative to UCam values, are displayed. One can see that the average difference between all groups' data (calculated between 87° and 90° SZA) is on the order of 4% with a scatter of 16%.

[41] Although moderately significant, the improved consistency of the IASB analyzed comparison points to the importance of features that are known to be treated differently by the individual analysis packages (e.g., wavelength calibration, Ring cross sections, offset corrections, and the Fraunhofer fit used by the Heidelberg group). Some groups appear to be more affected by this than others. In particular, the NILU and Heidelberg data appear to be brought more into agreement with the IASB analysis.

[42] Remaining differences between the groups' measurements are likely to be due to actual differences in the measured spectra rather than to the analyses. Part of the discrepancies between the groups may be due to different amounts of BrO in the reference spectra in each case. Although the specified reference spectrum was at a SZA of 70°, the closest available SZA spectrum was chosen by each group. In some cases this was as much as 0.5° SZA difference. Other more subtle factors are also likely to play a role, like differences in spectral quality, differences in the field of view that would lead to a different sensitivity to cloud effects and tropospheric ozone, and different sensitivities to factors like stray light and dark current. As mentioned in section 6.9, there is also probably a limit to the ability of the calibration routines to correctly determine the wavelength registration of the spectra. This may be on the order of 0.01 nm, which though small, is significant in an analysis as sensitive as that for BrO.

[43] Note, finally, that in general, the afternoon data are more scattered than the morning data. This is probably the result of instrument temperature regulation problems during the hotter afternoons, combined with increased NO_2 and cloud cover [*Pfeilsticker et al.*, 1999; *Winterrath et al.*, 1999].

10. Summary of Error Sources

[44] The various sources of errors that have been identified in this paper are summarized in Table 6. This includes an approximate assessment of the likely significance that such sources of error may have and estimates of the size of the errors based on the results of the various sensitivity studies described in section 6. Note that errors given here are not meant as a full error budget of the BrO retrieval. They are merely representative of the case for slant column differences calculated in the range 87°–90° SZA using a reference spectrum taken at 70° SZA, as determined from a limited though representative sample of five different instruments. Possible differences in sensitivity depending on the choice of the standard conditions and on atmospheric

Table 6. Summary of Some Possible Sources of Error in the Analysis For BrO in Zenith-Sky Spectra by the DOAS Technique[a]

Error Source	Comments	Error Estimate
Offset correction	moderate to large effect depending on individual characteristics of spectrometer	10–70%
Wavelength interval for fit	moderate to large effect	2–40%
I_0 correction	large effect	35%
BrO cross-section shift (0.17 nm)	significant effect	23%
O_3 temperature dependence	significant effect but well accounted for by fitting two O_3 cross sections of differing temperatures	25%
Spectral wavelength calibration	moderately significant effect that is at present limited to an accuracy of ~0.01 nm	18%
Slit function determination	moderate effect	10%
Degree of polynomials used	small effect	8%
O_3 cross-section shift (0.03 nm)	small if using I_0 correction and 346- to 359- nm fit window	5%
Low BrO cross-section resolution	small effect	4%
Wavelength-dependent air mass factor corrected O_3 cross sections	very small effect as long as accounting for O_3 temperature dependence in some other way, such as two O_3 cross-sections	3%
False fitting of BrO	very small effect provided I_0 corrected cross sections are used	–

[a]Relative importance of the sources has been assessed. Error estimates are for slant column differences calculated between 87° and 90° SZA using a reference spectrum at 70° SZA, as derived from results of sensitivity tests given in Table 5.

conditions (temperature, NO_2 amounts, cloud cover, and aerosols) cannot be ruled out.

11. Further Requirements

[45] In this study the inaccuracy of the wavelength calibration of the GOME spectra, now resolved [*Voigt et al.*, 2001], and of the O_4 spectra were shown to be significant sources of error in the retrieval of BrO. Even though for many of the gases, little rotational structure is expected in their vibronic spectra, this study indicates the need for accurate high spectral resolution measurements of the absorption cross sections of the gases covering a relevant atmospheric range of temperature and pressure. A database of accurate high-resolution gaseous absorption cross sections in the UV and visible spectral regions is expected to replace the GOME data set for remote sensing applications using the DOAS retrieval technique. New O_4 cross sections under more realistic atmospheric conditions have been measured and recently released [*Hermans et al.*, 2001], so their suitability should be assessed and recommendations should be made.

[46] Further attention should be given to the determination of Ring cross sections and offsets, as these appear to be significant sources of differences between the groups. In addition, improvements may be obtainable if the measurement of instrument slit functions can be improved. As far as further improvements in the analysis by the method of intercomparison are concerned, it would be desirable to have another such intercomparison under more suitable conditions, perhaps at somewhat higher latitude in winter when there is more BrO present and the temperatures are more conducive to the instruments functioning optimally.

12. Conclusions

[47] This study has highlighted the difficulty of BrO measurement and the extreme sensitivity of BrO DOAS retrieval to very small changes in calibration of spectra and cross sections as well as to the wavelength fitting window used for the analysis. As a consequence, there is a need for high-resolution cross sections with very accurate wavelength calibration and high signal-to-noise ratio in this region. Additionally, cross sections should be measured over a range of temperatures both to measure differences in cross-section shape and magnitude and to check for wavelength shifts with temperature. Given the nonideal nature of the measurements, a reasonably good agreement (to within some 4% on average between 87° and 90° SZA with a scatter of 16%) has been found under carefully controlled analytical conditions. As a result of the investigations into the sensitivity of the analysis to a number of factors, recommendations have been made as to the best analysis with the presently available cross sections.

[48] This study has demonstrated that consistent observations of BrO columns by a series of instruments operated by different groups can be obtained as long as carefully controlled common analysis settings are used. As shown in a recent study by *Sinnhuber et al.* [2002], the gain in data consolidation is such that the technique is now approaching the level of accuracy needed to allow modelers to assess our current understanding of stratospheric bromine chemistry.

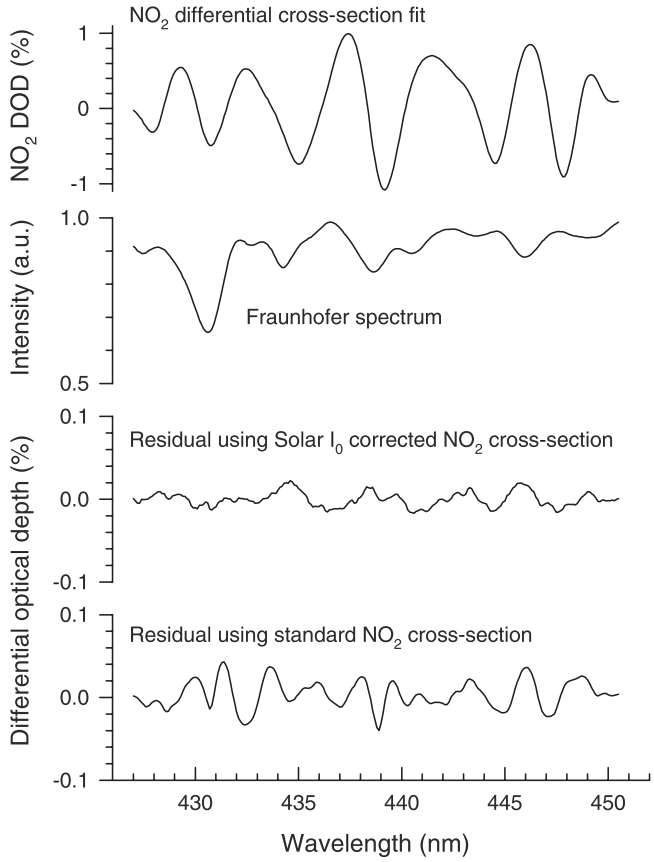

Figure A1. Results from a fit of NO_2 absorption cross sections to a NO_2 cell measurement performed in Lauder on 31 July 1996, using the zenith sky as a light source. The improvement in residuals obtained when applying a correction for the so-called I_0 effect (see text) is obvious.

Given that the intercomparison measurements were not made under the same conditions as the previously published measurements and that the error sources identified affect different instruments to different extents, the implications for the accuracy of previously published slant column measurements of BrO are difficult to assess. While it is likely that such data may be affected by a few percent to tens of percent, the error is not of an order of magnitude such that the main conclusions drawn in previous investigations should not be invalidated by the present study.

[49] Finally, an important application of the reported study might be the future development and exploitation of networked BrO observations as part of the Network for the Detection of Stratospheric Change (NDSC).

Appendix A

A1. Solar I_0 Effect

[50] The need to correct the convolved cross sections used in zenith-sky UV/visible spectroscopy actually arises because the I_0 spectrum in the zenith-sky measurements is the highly structured solar Fraunhofer spectrum, whereas the I_0 spectrum used to measure the laboratory absorption cross sections is usually nearly flat. In zenith-sky differential absorption spectroscopy, one removes the Fraunhofer

structures by forming the log ratio of a twilight spectrum to a reference midday spectrum, thus retaining the absorptions by atmospheric absorbers. However, because both of the spectra forming the ratio are measured by the instrument and therefore have been filtered by the instrument slit function before the ratio is calculated, complete removal of the Fraunhofer structures is not possible. This can be seen by looking at the integral equations given here.

[51] Assuming no absorption, the midday reference spectrum measured and therefore filtered by the instrument is

$$I_R(\lambda') = \int I_0(\lambda) W(\lambda - \lambda') d\lambda, \tag{A1}$$

where I is the spectrum measured by the zenith-sky spectrometer, I_0 is the solar Fraunhofer spectrum, and $W(\lambda)$ is the normalized instrument slit function. Similarly, the twilight spectrum also filtered by the instrument (where h is the optical depth of absorbers such as O_3 and NO_2) is

$$I(\lambda') = \int I_0(\lambda) e^{-h(\lambda)} W(\lambda - \lambda') d\lambda\,. \tag{A2}$$

[52] The negative log ratio of the twilight to the reference spectra does not completely remove the I_0 term unless $I_0(\lambda)$ or $h(\lambda)$ are constant over the integration interval (the full width of the instrument slit function). This essentially occurs for broadly structured cross sections such as, for example, those of O_3 for $\lambda > 400$ nm, but not for NO_2, BrO, OClO, or O_3 in the Huggins bands. The significance of the solar I_0 effect has been quantified using synthetic spectra and real spectra, as shown in Figures 2 and 5, respectively, and as discussed in sections 5 and 6.

A2. Correcting Absorption Cross Sections For the Solar I_0 Effect

[53] In order to generate absorption cross sections that include the solar I_0 effect in their shape, the method adopted in this work is to calculate synthetic spectra with an optical depth $h(\lambda) = \sigma(\lambda).X$, where $\sigma(\lambda)$ is the absorption cross section and X is the corresponding column amount. The correction depends slightly on the value of X, because of the nonlinear terms in the integral, so a value that is typical of the maximum measured is used. This leads to the following definition for the solar I_0-corrected cross section:

$$\sigma_{\text{corrected}}(\lambda') = -\frac{1}{X} \ln\left\{\frac{\int I_0(\lambda) \exp\left[-h(\lambda)\right]\ W(\lambda - \lambda') d\lambda}{\int I_0(\lambda)\ W(\lambda - \lambda') d\lambda}\right\}. \tag{A3}$$

[54] In this work the solar atlas by *Kurucz et al.* [1984] was used as the reference Fraunhofer spectrum (I_0). The significance of the correction is demonstrated in Figure A1, where an NO_2 cell fit residual (obtained using the zenith sky as a light source) is shown using standard uncorrected NO_2 cross sections and NO_2 cross sections corrected using (A3).

[55] **Acknowledgments.** Our thanks are owed to the staff at OHP and to A. Sarkissian and H. K. Roscoe for organizational and practical assistance. This exercise was funded by the European Commission through the SCUVS-3 and Stratospheric BrO projects (contracts ENV-CT95-0089 and ENV4-CT97-0521).

References

Aliwell, S. R., R. L. Jones, and D. J. Fish, Midlatitude observations of the seasonal variation of BrO, 1, Zenith-sky measurements, *Geophys. Res. Lett.*, *24*, 1195–1198, 1997.

Arpag, K. H., P. V. Johnston, H. L. Miller, R. W. Sanders, and S. Solomon, Observations of the stratospheric BrO column over Colorado, 40°N, *J. Geophys. Res.*, *99*, 8175–8181, 1994.

Avallone, L. M., D. W. Toohey, S. M. Schauffler, W. H. Pollock, L. E. Heidt, E. L. Atlas, and K. R. Chan, In situ measurements of BrO during AASE II, *Geophys. Res. Lett.*, *22*, 831–834, 1995.

Brion, J., C. D. Daumont, J. Malicet, and C. Parisse, High-resolution laboratory absorption cross-section of O_3: Temperature effect, *Chem. Phys. Lett.*, *213*, 610–612, 1993.

Brune, W. H., and J. G. Anderson, In situ observations of midlatitude stratospheric ClO and BrO, *Geophys. Res. Lett.*, *13*, 1391–1394, 1986.

Burrows, J. P., A. Richter, A. Dehn, B. Deters, S. Himmelmann, S. Voigt, and J. Orphal, Atmospheric remote-sensing reference data from GOME, 2, Temperature-dependent absorption cross-sections of O_3 in the 231–794 nm range, *J. Quant. Spectrosc. Radiat. Transfer*, *61*, 509–517, 1999.

Bussemer, M., Der Ring-Effekt: Ursachen und Einfluss auf die Messung stratophaerischer Spurenstoffe, diploma thesis, Inst. for Environ. Phys., Univ. of Heidelberg, Heidelberg, Germany, 1993.

Carroll, M. A., R. W. Sanders, S. Solomon, and A. L. Schmeltekopf, Visible and near-ultraviolet spectroscopy at McMurdo Station, Antarctica 6: Observations of BrO, *J. Geophys. Res.*, *94*, 16,633–16,638, 1989.

Chance, K., and R. J. D. Spurr, Ring effect studies: Rayleigh scattering including molecular parameters for rotational Raman scattering and the Fraunhofer spectrum, *Appl. Opt.*, *36*, 5224–5239, 1997.

Dahlback, A., and K. Stamnes, A new spherical model for computing the radiation field available for photolysis and heating at twilight, *Planet. Space Sci.*, *39*, 671–683, 1991.

Eisinger, M., A. Richter, A. Ladstaetter-Weissenmayer, and J. P. Burrows, DOAS zenith sky observations, 1, BrO measurements over Bremen (53°N) 1993–1994, *J. Atmos. Chem.*, *26*, 93–108, 1997.

Fish, D. J., R. L. Jones, and K. E. Strong, Midlatitude observations of the diurnal variation of stratospheric BrO, *J. Geophys. Res.*, *100*, 18,863–18,871, 1995.

Fish, D. J., S. R. Aliwell, and R. L. Jones, Midlatitude observations of the seasonal variation of stratospheric BrO, 2, Interpretation and modeling study, *Geophys. Res. Lett.*, *24*, 1199–1202, 1997.

Greenblatt, G. D., J. J. Orlando, J. B. Burkholder, and A. R. Ravishankara, Absorption measurements of oxygen between 330 and 1140 nm, *J. Geophys. Res.*, *95*, 18,577–18,582, 1990.

Harder, H., et al., Stratospheric BrO profiles measured at different latitudes and seasons: Atmospheric observations, *Geophys. Res. Lett.*, *25*, 3843–3846, 1998.

Harder, J. W., J. W. Brault, P. V. Johnston, and G. H. Mount, Temperature-dependent NO_2 cross sections at high spectral resolution, *J. Geophys. Res.*, *102*, 3861–3879, 1997.

Hermans, C., A. C. Vandaele, B. Coquart, A. Jenouvrier, M.-F. Mérienne, S. Fally, M. Carleer, and R. Colin, Absorption bands of O_2 and its collision-induced bands in the 30,000–7500 cm^{-1} wavenumber region, in *IRS 2000: Current Problems in Atmospheric Radiation*, edited by W. L. Smith and Y. M. Timofeyev, pp. 639–642, A. Deepak, Hampton, Va., 2001.

Kreher, K., P. V. Johnston, S. W. Wood, B. Nardi, and U. Platt, Ground-based measurements of tropospheric and stratospheric BrO at Arrival Heights, Antarctica, *Geophys. Res. Lett.*, *24*, 3021–3024, 1997.

Kurucz, R. L., I. Furenlid, J. Brault, and L. Testerman, Solar flux atlas from 296 nm to 1300 nm, *Natl. Sol. Obs. Atlas 1*, 239 pp., Harvard Univ., Cambridge, Mass., 1984.

Marquard, L. C., T. Wagner, and U. Platt, Improved air mass factor concepts for scattered radiation differential optical absorption spectroscopy of atmospheric species, *J. Geophys. Res.*, *105*, 1315–1327, 2000.

McKinney, K. A., J. M. Piersen, and D. W. Toohey, A wintertime in situ profile of BrO between 17 and 27 km in the Arctic vortex, *Geophys. Res. Lett.*, *24*, 853–856, 1997.

Otten, C., F. Ferlemann, U. Platt, T. Wagner, and K. Pfeilsticker, Ground-based DOAS UV/VIS measurements at Kiruna (Sweden) during the SESAME winters 1993/94 and 1994/95, *J. Atmos. Chem.*, *30*, 141–162, 1998.

Pfeilsticker, K., et al., Intercomparison of the detected influence of tropospheric clouds on UV-visible absorptions detected during the NDSC intercomparison campaign at OHP in June 1996, *Geophys. Res. Lett.*, *26*, 1169–1172, 1999.

Pundt, I., La distribution verticale de BrO et IO dans la basse stratosphère: Mesure et interprétation, Ph.D. thesis, Univ. de Pierre et Marie Curie, Paris, France, 1997.

Pundt, I., J.-P. Pommereau, F. Goutail, M. P. Chipperfield, F. Danis, N. R. P. Harris, and J. A. Pyle, Vertical distributions of BrO and Br_y at high, mid-, and low latitudes, paper presented at Fifth European Workshop on Stratospheric Ozone, St. Jean de Luz, France, 27 September through 1 October 1999, *EUR 19340*, p. 324–327, Univ. Pierre et Marie Curie, Paris, 2000.

Richter, A., Ground-based UV/VIS measurements of stratospheric trace gases above Bremen (53°N), Ph.D. thesis, Univ. of Bremen, Bremen, Germany, 1997.

Richter, A., M. Eisinger, A. Ladstaetter-Weissenmayer, and J. P. Burrows, DOAS zenith sky observations, 2, Seasonal variation of BrO over Bremen (53°N) 1994–1995, *J. Atmos. Chem.*, *32*, 83–89, 1999.

Roscoe, H. K., et al., Slant column measurements of O_3 and NO_2 during the NDSC intercomparison of zenith-sky UV-visible spectrometers in June 1996, *J. Atmos. Chem.*, *32*, 281–314, 1999.

Sinnhuber, B.-M. A., et al., The global distribution of stratospheric bromine monoxide: Intercomparison of measured and modeled slant column densities, *J. Geophys. Res.*, *107*, 10.1029/2001JD000940, in press, 2002.

Solomon, S., A. L. Schmeltekopf, and R. W. Sanders, On the interpretation of zenith-sky absorption measurements, *J. Geophys. Res.*, *92*, 8311–8319, 1987.

Tørnkvist, K. K., D. W. Arlander, and B.-M. Sinnhuber, Ground-based UV measurements of BrO and OClO over Ny-Ålesund during winter 1996 and 1997 and Andøya during winter 1998/99, *J. Atmos. Chem.*, in press, 2002.

Van Daele, A.-C., C. Hermans, P. C. Simon, M. Carleer, R. Colin, S. Fally, M.-F. Merienne, A. Jenouvrier, and B. Coquart, Measurements of the NO_2 absorption cross-section from 42,000 cm^{-1} to 10,000 cm^{-1} (238–1000 nm) at 220 K and 294 K, *J. Quant. Spectrosc. Radiat. Transfer*, *59*, 171–184, 1998.

Van Roozendael, M., C. Fayt, C. Hermans, and J.-C. Lambert, Ground-based UV-visible measurements of BrO, NO_2, O_3, and OClO at Harestua (60°N) since 1994, in *Polar Stratospheric Ozone 1997: Proceedings of the 4th European Symposium on Stratospheric Ozone Research*, *Eur. Comm. Air Pollut. Res. Rep. 66*, edited by N. R. P. Harris, I. Kilbane-Dawe, and G. T. Amanatidis, pp. 510–513, 1998.

Voigt, S., J. Orphal, K. Bogumil, and J. P. Burrows, Temperature dependent absorption cross sections of O_3 in the 230–850 nm region, measured by Fourier transform spectroscopy, *J. Photochem. Photobiol. A*, *143*, 1–9, 2001. (Available from http://www.iup.physik.uni-bremen.de/gruppen/molspec/index.html.)

Vountas, M., V. V. Rozanov, and J. P. Burrows, Ring effect: Impact of rotational Raman scattering on the radiative transfer in Earth's atmosphere, *J. Quant. Spectrosc. Radiat. Transfer*, *60*, 943–961, 1998.

Wagner, T., H. Haug, L. Marquard, E. Scheer, and U. Platt, Errors of stratospheric DOAS measurements due to the wavelength dependence of the air mass factor and the incorrect removal of Fraunhofer lines, GOME Geophysical Validation Campaign, paper presented at Final Results Workshop, Eur. Space Agency, Eur. Space Res. Inst., Frascati, Italy, 1996.

Wahner, A., A. R. Ravishankara, S. P. Sander, and R. R. Friedl, Absorption cross-section of BrO between 312 and 385 nm at 298 and 223 K, *Chem. Phys. Lett.*, *152*, 507–510, 1988.

Wilmouth, D. M., T. F. Hanisco, N. M. Donahue, and J. G. Anderson, Fourier transform ultraviolet spectroscopy of the $A(^2\Pi_{3/2}) \leftarrow \times(^2\Pi_{3/2})$ transition of BrO, *J. Phys. Chem.*, *103*, 8935–8944, 1999.

Winterrath, T., T. P. Kurosu, A. Richter, and J. P. Burrows, Enhanced O_3 and NO_2 in thunderstorm clouds: Convection or production?, *Geophys. Res. Lett.*, *26*, 1291–1294, 1999.

S. R. Aliwell and R. L. Jones, Centre for Atmospheric Science, Department of Chemistry, University of Cambridge, Lensfield Road, Cambridge CB2 1EW, UK. (simon@atm.ch.cam.ac.uk; rlj1001@cus.cam.ac.uk)

D. W. Arlander and K. K. Tørnkvist, Norwegian Institute for Air Research, Instituttveien 18, N-2007, Kjeller, Norway. (bill.arlander@nilu.no; kjersti.toernkvist@nilu.no)

J. P. Burrows and A. Richter, Institute of Environmental Physics, University of Bremen, P.O. Box 330440, 28334 Bremen, Germany. (burrows@iup.physik.uni-bremen.de; richter@iup.physik.uni-bremen.de)

D. J. Fish, Department of Meteorology, University of Reading, Early Gate, PO Box 243, Reading RG6 6BB, UK. (D.J.Fish@reading.ac.uk)

P. V. Johnston, National Institute of Water and Atmospheric Research, Private Bag 50061, Omakau, Otago Lauder, State Highway 85, Central Otago, New Zealand 9182. (p.johnston@niwa.cri.nz)

J. C. Lambert and M. Van Roozendael, Institut d'Aéronomie Spatiale de Belgique, Avenue Circulaire 3, B-1180, Brussels, Belgium. (lambert@oma.be; michelv@oma.be)

K. Pfeilsticker and T. Wagner, Institute of Environmental Physics, University of Heidelberg, INF 366, D-69120 Heidelberg, Germany. (Klaus.Pfeilsticker@iup.uni-heidelberg.de; Thomas.Wagner@iup.uni-heidelberg.de)

I. Pundt, Service d'Aéronomie du CNRS, BP 3, F-91371 Verrières-le-Buisson, France. (irene.pundt@aerov.jussieu.fr)